

1 **A simplified component-based methodology for the seismic vulnerability**
2 **assessment of school buildings using nonlinear static procedures: application to**
3 **RC school buildings**
4

5 Rafael Fernández¹, Luis Yamin¹, Dina D’Ayala², Rohit Adhikari², Juan C. Reyes¹, Juan Echeverry¹,
6 Gustavo Fuentes¹

7 ¹Department of Civil and Environmental Engineering, Universidad de los Andes, Bogotá, Colombia

8 ²Department of Civil and Geomatic Engineering, University College London, London, U.K.

9 **Corresponding Author:**

10 Rafael Fernández

11 Email: ri.fernandez1110@uniandes.edu.co

12 **Abstract:**

13 Several earthquakes have affected school infrastructure, compromising the safety of students and all
14 the educational community. These damages are not caused solely by the action of earthquakes, but
15 also by the lack of adequate seismic design, deficient construction practices, and lack of regulations
16 and normative to ensure an appropriate quality for infrastructure. Therefore, to analyze how is the
17 expected infrastructure behavior in earthquakes, this study presents a simplified methodology for the
18 seismic vulnerability assessment of school buildings. The methodology includes several components:
19 data collection, the characterization of Index Buildings (IB), hazard definition, nonlinear numerical
20 modeling of the structural response, seismic performance assessment and the vulnerability integration
21 using a component-based approach. The novelty of the proposed methodology resides in the fact of
22 its simplicity and robustness obtained by combining a simplified non-linear incremental static
23 analysis together with a component-based vulnerability derivation methodology to assess the
24 behavior of school buildings. This methodology is applied to a set of 11 Reinforced Concrete (RC)
25 school building types representing common structural systems and seismic design levels. A number
26 of sensitivity analyses are also carried out, varying the geometry, the foundation-soil flexibility, the
27 mechanical properties of infill masonry walls, the non-structural elements and the analysis type,
28 showing the versatility and reliability of the proposed methodology.

29 **Key words:** seismic vulnerability, non-linear static procedures, reinforced concrete buildings, school
30 buildings

31 **1 Introduction**

32 Quality education is a priority established in the Sustainable Development Goals (SDG) in which the
33 fourth goal corresponds to "Ensure inclusive and equitable quality education and promote lifelong
34 learning opportunities for all" (United Nations 2015). One of the most important factors to achieve
35 this goal is to ensure safer infrastructure, which is widely promoted by multilateral agencies through
36 programs at the regional level with various objectives. Indeed, UNESCO has emphasized
37 infrastructure safety by developing VISUS (UNESCO 2019), a methodology for assessing safety
38 attributes in school facilities with applications in El Salvador, Laos, Indonesia, and Peru. The
39 UNISDR (the United Nations Office for Disaster Risk Reduction), in collaboration with the Global
40 Alliance for Disaster Risk Reduction & Resilience in Education Sector (GADRRRES), has also
41 developed programs and action plans such as the Comprehensive School Safety program and the
42 Worldwide Initiative for Safe Schools (UNDRR 2017). These two initiatives provide a global
43 framework to support activities related to safe learning facilities, school disaster risk management,
44 and risk reduction and resilience in education. Moreover, since 2014, the Global Program for Safer
45 Schools (GPSS) of the World Bank is actively engaged in developing roadmap and guidelines, as
46 well as assisting governments in developing countries, to reduce the disaster risk to school
47 infrastructure. The main purpose of GPSS is to boost large-scale investments to enhance the safety
48 and resilience of school infrastructure at risk from natural hazards and contribute to improving the
49 quality of learning environments for children (The World Bank 2019).

50 School safety is threatened by several natural hazards such as earthquakes, cyclones, floods, wildfires,
51 and landslides, imposing risk for children. Among these hazards that impact school infrastructure,
52 earthquakes pose the greatest risk and thus the present study focuses on seismic vulnerability. Some
53 of the most recent examples of damages due to earthquakes evidenced in Latin American
54 infrastructure can be found in the Geotechnical Extreme Events Reconnaissance (GEER) reports for
55 Ecuador 2016 and Mexico 2017 (GEER 2016, 2017). As reported by Earthquake Engineering
56 Research Institute (EERI), earthquakes have also caused vast damage in other regions of the world,
57 such as India, Indonesia, Peru, and Turkey (EERI 2019). In particular, in Nepal, the 2015 Gorkha
58 earthquake showed the high vulnerability of school building with different structural systems, such
59 as reinforced concrete frames, cement-bonded and mud-bonded masonry, and timber frames among
60 others (Chen et al. 2017). However, it is essential to note that earthquakes themselves have not caused
61 the disaster, but this occurred primarily due to the lack of adequate construction practices through
62 regulations and infrastructure of appropriate quality (IADB 2014; UNDRR 2017; Nassirpour et al.
63 2018; The World Bank 2019). Based on the underlying weakness, or vulnerability condition of
64 children due to their age and response capacities, governments have a direct responsibility in reducing
65 the physical vulnerability of school infrastructure (D'Ayala et al. 2020).

66 The first step towards reducing the structural vulnerability of school infrastructure is the assessment
67 of its structural and damage behavior to understand the expected performance during possible
68 earthquakes. For this, simplified methodologies to develop safety index can be implemented such as
69 the Rapid Visual Screening (RVS) method proposed by Ruggieri et al (2020). In this method, the
70 authors propose to obtain in-field data related to structural and non-structural components,
71 organizational characteristics, and the number of occupants to generate a composite safety index.
72 RVS approaches however have limited applicability when needing to identify strengthening strategies

73 for specific typologies. In this respect fragility functions and vulnerability functions, derived on the
74 basis of analytical models, are more suitable tools for assessing the seismic safety of buildings (Masi
75 2003; D'Ayala 2013; Michel et al. 2014). Fragility functions represent the probability of exceeding a
76 damage state of a specific structure type given the hazard intensity measure (D'Ayala et al. 2015).
77 On the other hand, vulnerability functions represent the overall probability of damage for a structure,
78 expressed such as the Mean Damage Ratio (MDR), and its variance given a hazard intensity measure,
79 such as the Peak-Ground Acceleration (PGA) or the Spectral Acceleration (S_a) (Yamin et al. 2014).
80 The MDR is usually expressed in economic terms, as the ratio of the expected total repair cost to the
81 building's total replacement cost (Yamin et al. 2017). The building's total replacement cost is defined
82 as the actual reconstruction cost of the building according to local price conditions in the region under
83 analysis. Most common hazard intensity measures for seismic fragility and vulnerability assessment
84 are the PGA or $S_a(T_1)$, while other intensity measures such as Spectral Displacement (S_d) are also
85 used in practice. The choice of IM depends on the typology of the building under assessment (Yamin
86 et al. 2017).

87 Recent studies have proposed diverse yet independent or isolated methodologies for the seismic
88 Vulnerability or Fragility (V/F) assessment of representative buildings (Dolšek and Fajfar 2005;
89 Dolšek 2012; Abo-El-ezz et al. 2013; D'Ayala et al. 2015; Del Gaudio et al. 2015; Hosseinpour and
90 Abdelnaby 2017; Yamin et al. 2017; Cremen and Baker 2019). Approaches may consider empirical,
91 expert opinion-based, analytical or hybrid methods to derive vulnerability or fragility functions
92 (Porter et al. 2002; D'Ayala et al. 2015; Silva et al. 2018). The analytical vulnerability approach
93 allows for an unbiased and consistent assessment that has proven to be applicable worldwide,
94 independently of historical seismic damage data and local expertise on specific building performance
95 (Silva et al. 2018). The analytical methods allow V/F functions to be easily updated, complemented,
96 and modified as more refined data on exposure or refined analytical approaches become available. In
97 addition, the analytical approach considers region-specific characteristics such as the hazard
98 specifications, local geographical seismic conditions, and local characteristics, generating more
99 reliable vulnerability curves.

100 Recent studies on vulnerability and resilience of school portfolios, increasingly apply analytical
101 vulnerability approaches considering local characteristics of buildings. Indeed, Samadian et al (2019)
102 present a new methodology based on regional economic conditions for loss estimation used to derive
103 vulnerability functions in a broader framework to assess resilience in school buildings in Iran.
104 Similarly, Gonzalez et al (2020) provide a methodology to quantify seismic resilience in Mexico
105 City school facilities. In this methodology, the physical and human vulnerability functions are derived
106 to develop, in a next step, a recovery function to assess resilience. An approach applied to Nepal
107 school portfolio, developed by Giordano et al (2020), characterize the out-of-plane response of
108 unreinforced masonry buildings. Despite these current developments and additional efforts such as
109 methods proposed in literature (Michel et al. 2014; Rossetto et al. 2014; Yamin et al. 2014; Mora et
110 al. 2015; Silva et al. 2018) there is a lack of a technically robust and comprehensive yet simple
111 methodology to assess the vulnerability of school building aggregate at scale, for example at regional
112 or national level, economically and reliably.

113 To address the need of a comprehensive yet simple methodology for assessing the seismic
114 fragility/vulnerability of school buildings, this study presents an efficient and reliable methodology
115 to assess seismic vulnerability in Reinforced Concrete (RC) school buildings, based on the definition

116 of a comprehensive taxonomic characterization for the development of index buildings and estimation
117 of simplified seismic vulnerability functions using a component-based approach. The proposed
118 methodology is part of the developments made in the Global Library of School Infrastructure
119 (GLOSI) framework of the GPSS, funded by the Global Facility for Disaster Reduction and Recovery
120 (GFDRR) of the World Bank. GLOSI is a global library of data and information related to school
121 infrastructure as well as methodologies and tools for assessing and reducing the associated
122 vulnerability (The World Bank 2019). It is comprised by a global catalogue of school building types,
123 generic vulnerability information and retrofitting solutions that can be implemented at large-scale
124 level (The World Bank 2019). The paper is organized as follows: section 2 presents the details of the
125 proposed simplified vulnerability assessment methodology. Section 3 presents a case study
126 application in the global GLOSI index buildings. Section 4 develops a sensitivity analysis varying
127 different parameters to understand the versatility and reliability of the methodology and its advantages
128 for future use of vulnerability in risk assessments of school infrastructure. For the sensitivity analysis,
129 the geometrical variations, foundation-soil flexibility, quality of masonry infills, non-structural
130 vulnerable elements and the analysis type are considered. Even though we acknowledge that some
131 buildings in a school facility may have horizontal and vertical irregularities in cases of kitchens,
132 canteens, administrative or mixed-use buildings, the focus of this study are the RC schools buildings
133 used for classrooms only, where the students spend most of their time. These buildings are mostly
134 regular in plan and elevation, as identified in the SIDA report in Nepal (Digicon Engineering Consult
135 and The World Bank 2016) and more globally in the GLOSI (The World Bank 2019). Finally, section
136 5 presents the summary and conclusions.

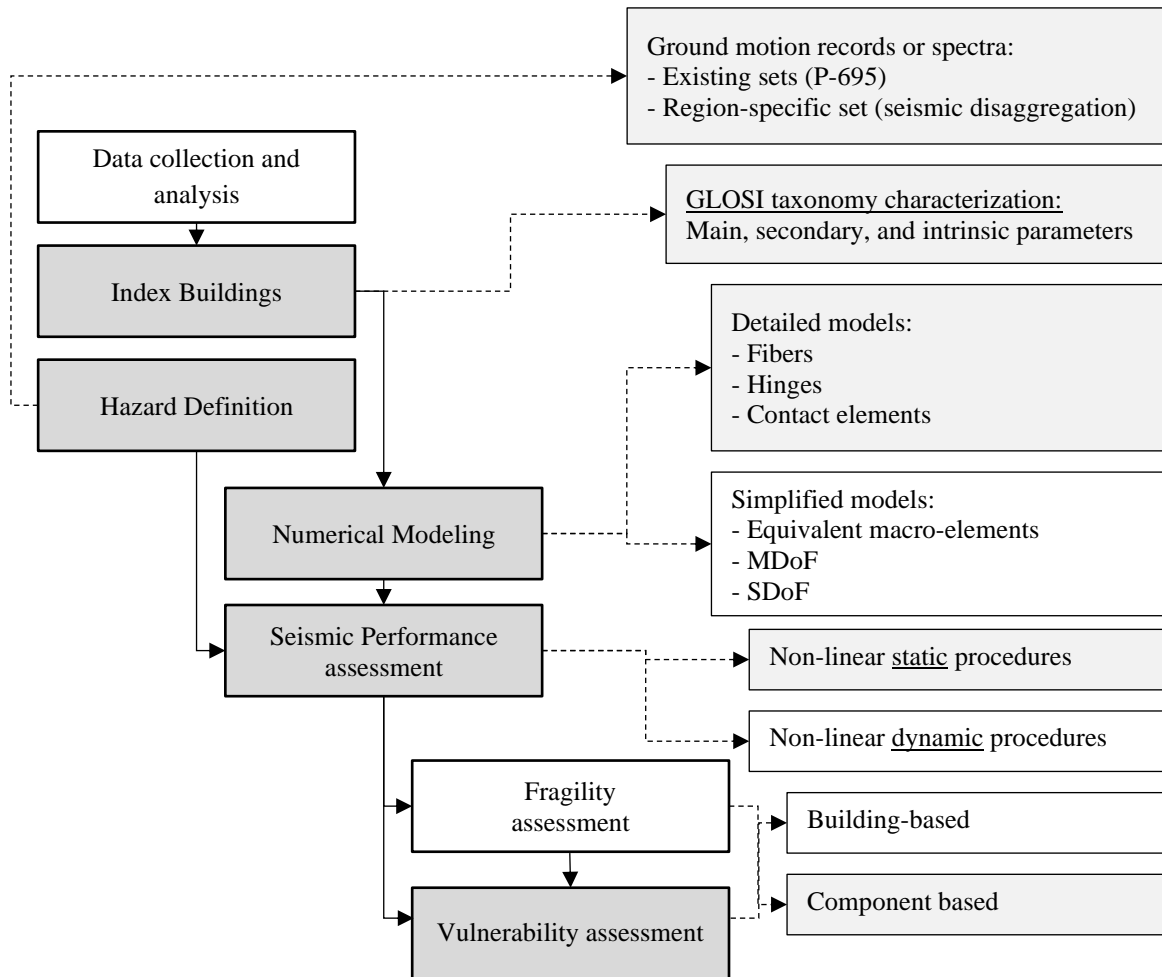
137

138 **2 Proposed methodology for the simplified vulnerability assessment**

139 The methodology presented herein aims to develop simplified seismic vulnerability functions using
140 a component-based approach for low and mid-rise school buildings (1 to 3 stories). The methodology
141 focuses on RC buildings, since this is one of the most common structural materials found in school
142 infrastructure. However, the methodological approach is also applicable to other structural systems
143 and materials. Indeed, a parallel study has been developed for masonry structures and details are
144 available in Adhikari (2021), Vatteri & D’Ayala (2021) and GLOSI (The World Bank 2019). Fig. 1
145 summarizes the main steps of the proposed methodology to derive vulnerability functions. The
146 methodology is comprised of six main steps: data collection, index buildings characterization, hazard
147 assessment, numerical modeling, seismic performance assessment, and vulnerability integration. The
148 data collection process and typology characterization is a substantial methodological endeavor in its
149 own right, as reported in GLOSI (The World Bank 2019), while the present manuscript concentrate
150 on the seismic performance assessment and vulnerability function derivation.

151 The first two steps are the data collection and the definition of Index Buildings (IBs). The data
152 collection is one of the most time and cost consuming tasks since institutional repositories do not
153 usually collect information related to structural characteristics of school buildings. There are several
154 methodologies to obtain information, such as field surveys, distance surveys, satellite images, proxies
155 based on limited existing databases, or combinations of these (Aleskerov et al. 2005; Prasad et al.
156 2009; Gunasekera et al. 2015; Fernández et al. 2021). The identification of representative index

157 buildings stems from the statistical analysis of the collected data. By applying the entire GLOSI
 158 taxonomy string to a large number of buildings, the most common combinations of parameters
 159 emerge, identifying recurring IBs. Once these are identified, intrinsic parameters, i.e., geometry and
 160 materials characteristics, should also be determined for each IB for modelling purposes. The GLOSI
 161 system has a number of predefined IBs that can be used to compare with the country specific data.
 162 Further information can be found in D’Ayala et al (2020) and The World Bank (2019).
 163



164
 165 **Fig. 1** Proposed simplified vulnerability assessment methodology – In dark grey the steps followed in this
 166 study

167 Once the IBs are fully characterized, the next step of the methodology is the seismic hazard definition.
 168 This may be selected using different techniques as the conditional mean spectrum (Baker 2011) or
 169 the uniform hazard spectrum (ASCE and SEI 2017a). However, these methodologies depend on a
 170 site-specific knowledge of the seismic conditions, which is seldom known in most countries. For a
 171 generalized and broader perspective, the hazard may be defined in terms of the
 172 acceleration/displacement spectra of the far-field set of earthquake ground motion records given by
 173 FEMA P-695 (ATC 2009) or other similar regional repositories. In particular, the FEMA P695 ground
 174 motion set is built to meet the following objectives: “to represent strong ground motions, to be

175 statistically representative, broadly applicable for collapse evaluation of various structural systems
176 and broadly applicable to structures at unknown location” (ATC 2009). Even though this set is
177 primarily recommended by FEMA to assess the collapse fragility of buildings through an Incremental
178 Dynamic Analysis (IDA), it can also be utilized to analyze lower damages states and corresponding
179 losses, as well as to be used in an Incremental Static Analysis (ISA) (Dolšek and Fajfar 2004; Gogus
180 and Wallace 2015; Ezzeldin et al. 2016). Also, its replicability, easy access and generic
181 characteristics, not linked to a specific area, make suitable to be used in the present study and within
182 the global remit of the GLOSI. Nonetheless, any set of appropriate ground motions specific to a
183 location, obtained from literature databases such as the PEER Strong Ground Motion Databases
184 (PEER 2020a), or by synthetic generation, can replace the current choice.

185 The next step of the methodology is the numerical modeling of the IBs. The modeling main objective
186 is to develop the pushover curve of the IB in the most critical direction. This numerical model should
187 be nonlinear and three-dimensional to characterize the structural behavior. To this end, depending on
188 the complexity of the structure analyzed and the identified failure modes, both plastic hinges or
189 distributed plasticity can be used, following internationally accepted methodologies (Mander et al.
190 1988; Elwood 2004; ATC 2005; Ibarra et al. 2005; ASCE and SEI 2017b; Di Trapani et al. 2018).
191 Any acceptable software can be used for the pushover curve derivation. Common computer software
192 available to perform this analysis are SAP2000, ETABS, Perform3D and OpenSees among others
193 (CSI Computer & Structures Inc 2004, 2016, 2020; PEER 2020b). It is important to note that this
194 methodology is limited to the most critical unidirectional analysis, the consideration of bidirectional
195 or vertical effects are out of the scope of this paper.

196 The pushover curve developed in the previous step will be used to derive the seismic performance
197 assessment. For this, an Incremental Static Analysis (ISA) is proposed which employs the latest
198 version of the N2 method in a set of incremental ground motions spectra (as in IDA analysis) (Fajfar
199 2000; Vamvatsikos and Cornell 2002; D’Ayala et al. 2015). This ISA methodology (Mwafy and
200 Elnashai 2001; Dolšek and Fajfar 2005), shows a good correlation with IDA methods for RC
201 buildings with and without masonry infills. The N2 methodology may be summarized as follows: for
202 each IB, the multiple degrees of freedom (MDOF) pushover curves are converted to a bilinear
203 idealized pushover curve of the equivalent single degree of freedom system (SDOF) following
204 standard engineering practices. This pushover is intersected with the inelastic demand spectrum for
205 each different ground motion in the selected set (scaled to different intensity measure values) to
206 generate several seismic performance points as Engineering Demand Parameters (EDP). The inelastic
207 response is calculated for a 5% damped elastic response spectrum, considering a ductility factor.
208 These results are expressed as a relation between the intensity measure (IM) and the corresponding
209 EDP. This methodology has been recommended by the Eurocode-8 (European Committee for
210 Standardization 2004) and have the advantage that its implementation for the determination of the
211 performance point is relatively easy. More details on this can be found in D’Ayala et al. (2015).

212 Other simplified methodologies available in the literature may be used to perform the nonlinear
213 seismic analysis, such as Fishbone (Nakashima et al. 2002; Qu et al. 2019), UMRHA (Chopra and
214 Goel 2002; Li and Ellingwood 2005), and others (Miranda 1999; Miranda and Akkar 2006) which
215 apply simplified models. The selection of one option over another depends on different factors, such
216 as purpose of the analysis, the acceptable level of uncertainty, the availability of resources, and the
217 data available (ATC 2005). An efficient nonlinear seismic analysis with reduced computational effort

218 as well as resources, while able to minimize the effect of uncertainties is favored for simplified
219 vulnerability assessment. The modelling uncertainty, according to FEMA 440, is due to the following
220 two components: the seismic analysis and the structural model. In the first case, the seismic analysis
221 could be performed using a pushover analysis or a response history analysis, where the highest
222 accuracy is obtained with a non-linear response history analysis. The proposed ISA methodology is
223 particularly efficient and accurate in the case of school infrastructure considering its geometric and
224 structural characteristics (regular and low- to mid-rise). For the second type of uncertainty, the
225 structural model could be represented as Single-Degree of Freedom (SDOF) or Multiple Degree of
226 Freedom (MDOF) models. The main consequence of simplifying the structural model using a SDOF
227 instead of a MDOF is that it lacks the representation of realistic failure modes or the interaction
228 between components. For this reason, the proposed methodology includes MDOF detailed model to
229 consider all these aspects, analyzed using the ISA methodology.

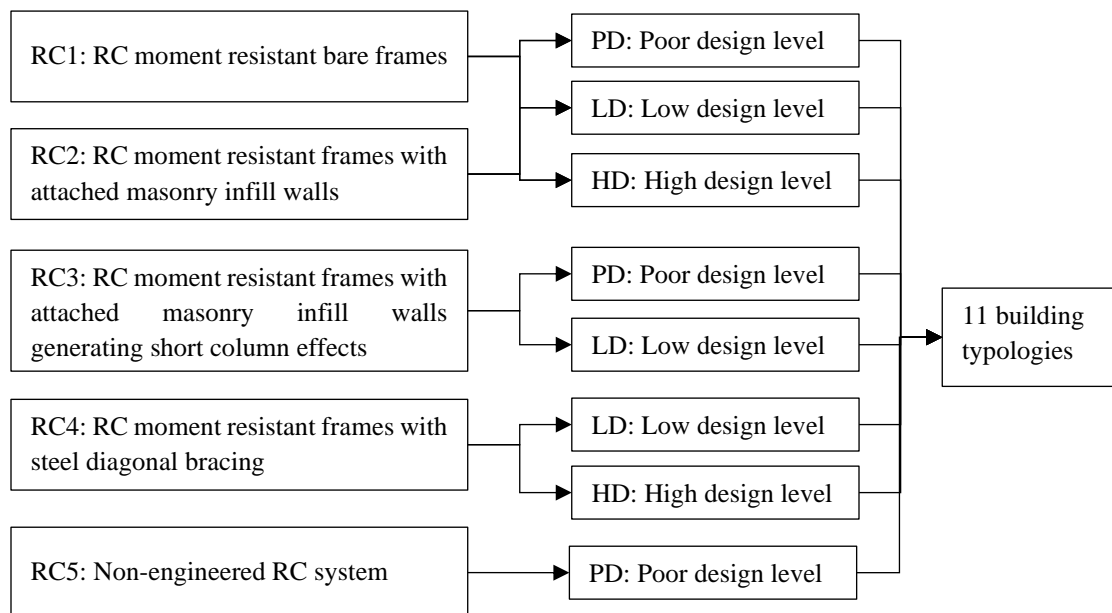
230 With the resulting EDPs, the final step is the derivation of vulnerability functions. It is important to
231 note that the development of functions should consider a wide range of uncertainties that depend on
232 the quality of the available information and the types of models and analyses used in each assessment
233 (Porter et al. 2002; Wen et al. 2003; D'Ayala et al. 2015; Silva 2019). In seismic vulnerability
234 assessment, the uncertainty is associated to seismic input, numerical modeling, material properties,
235 damage states, costs modeling and others (Yamin et al. 2017). These uncertainties can be
236 characterized as random or epistemic (Kiureghian and Ditlevsen 2009; D'Ayala et al. 2015). Random
237 uncertainties are associated with the seismic input, the soil response, the frequency content of the
238 seismic records used, and the variability in the materials and design of the building stock. Epistemic
239 uncertainty is associated with a lack of knowledge from a physical or engineering point of view,
240 limitation of the numerical modeling methodology, the estimation of the damage states, the repair
241 cost estimation, and other analytical parameters used in the assessment (Yamin et al. 2017). All
242 uncertainties are represented in the probability distribution function of each damage state of the
243 fragility functions or in the variance function indicated for the vulnerability function (which also
244 depends on the seismic intensity level). To consider and propagate the uncertainty through the
245 vulnerability functions, different methodologies considering the variability of EDP are represented
246 by a probabilistic distribution with an uncertainty β (ATC 2012; D'Ayala et al. 2015; Rincon et al.
247 2017). Therefore, the derivation is carried out using a component-based methodology following the
248 approach proposed by Yamin et al. (Yamin et al. 2017). This entails a model based on damage-
249 susceptible components, either structural or non-structural, which convolves the repair to replacement
250 cost ratios and the cumulative probability of damage expressed through the fragility functions. The
251 uncertainties and randomness of the variables are accounted for by performing a Monte Carlo
252 simulation. The method is further improved by implementing a more efficient seismic analysis
253 developed through the ISA assessment. The result of the methodology is a vulnerability function for
254 the analyzed building, including the mean damage ratio and the corresponding variance at each
255 intensity level. It is important to note that the building-based approach can also be used to develop
256 the vulnerability functions even though the authors recommend using a component-based approach
257 for its flexibility to include structural and non-structural components.

258

259 **3 Study case application**

260 *3.1 GLOSI RC index buildings*

261 The methodology described above was applied to a set of reinforced concrete Index Buildings (IBs)
262 in the GLOSI catalog (The World Bank 2019; D’Ayala et al. 2020). These IBs were selected to be
263 two-story buildings in the mid-rise (MR) category (one story is considered low-rise and two- and
264 three-story buildings are classified as mid-rise in GLOSI framework since school buildings usually
265 do not have more than 4 stories). This category was selected based on the distribution of the number
266 of stories of RC school buildings in developing countries such as Peru, Nepal, the Philippines and the
267 Dominican Republic (Nassirpour et al. 2018; The World Bank 2019). Five RC structural typologies
268 with different lateral resisting systems leading to various failure modes are considered for the
269 analysis: RC moment resistant bare frames (RC1) with light infill panels; RC moment resistant frames
270 with connected masonry infill walls (RC2); RC moment resistant frames with reduced height of
271 masonry infill walls generating short column effects (RC3); RC moment resistant frames with steel
272 bracing (RC4); and non-engineered RC systems where no frames are designed, usually a thin concrete
273 slab connect the columns, and are usually built by the community without following any building
274 code (RC5). Each structural system is evaluated for poor, low, or high design levels, as shown in Fig.
275 2. For illustration purposes, Fig. 3 presents the characteristic geometry of each structural system
276 considered. It is important to note that RC1 typology does not include any masonry walls or partitions
277 to present its moment-frame structural behavior as is. However, it is common to find actual RC1
278 typologies in the field with light partitions or masonry walls with sufficient separation from the
279 structural elements. All structural models were defined with the same geometry characteristics for
280 consistency in the results and comparisons.



281

282 **Fig. 2** Case study typologies

283



284 **Fig. 3** Geometry of selected typologies

285 In addition to the structural characteristics presented above, each building was characterized by a
 286 taxonomy string using the GLOSI classification system, developed by the authors for The World
 287 Bank (The World Bank 2019). The secondary parameters were fixed for all the eleven buildings with
 288 the following considerations: rigid diaphragm (RD), no irregularities (NI), long span –corresponding
 289 to typical classroom geometric configuration– (LS), regular column –strong column weak beam
 290 frame configuration– (RO), rigid foundation (RF), no pounding risk (NP), original structure (OS),
 291 good condition (GC) and vulnerable nonstructural elements (VN) (such as parapets, gables,
 292 bookshelves and others to consider the additional damage cost, while nonstructural members which
 293 interact with the main structure are explicitly included in the structural system modelling). Table 1
 294 presents the list of building typologies considered. The results described in this study are presented
 295 in reference to the Building Type string found in Table 1.

296 **Table 1** Taxonomy of the RC Index Buildings currently available in the GLOSI library

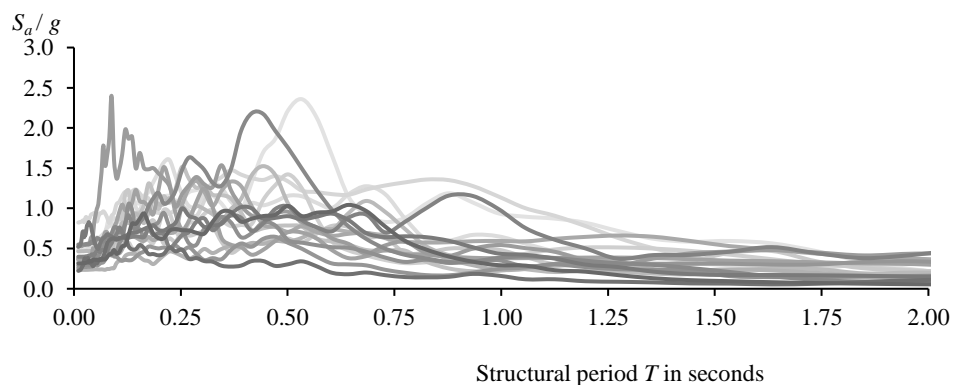
ID	Building Type	Index Building
1	RC1/MR/PD	RC1/MR/PD/RD/NI/LS/RO/RF/NP/OS/GC/VN
2	RC1/MR/LD	RC1/MR/LD/RD/NI/LS/RO/RF/NP/OS/GC/VN
3	RC1/MR/HD	RC1/MR/HD/RD/NI/LS/RO/RF/NP/OS/GC/VN
4	RC2/MR/PD	RC2/MR/PD/RD/NI/LS/RO/RF/NP/OS/GC/VN
5	RC2/MR/LD	RC2/MR/LD/RD/NI/LS/RO/RF/NP/OS/GC/VN
6	RC2/MR/HD	RC2/MR/HD/RD/NI/LS/RO/RF/NP/OS/GC/VN
7	RC3/MR/PD	RC3/MR/PD/RD/NI/LS/RO/RF/NP/OS/GC/VN
8	RC3/MR/LD	RC3/MR/LD/RD/NI/LS/RO/RF/NP/OS/GC/VN
9	RC4/MR/LD	RC4/MR/LD/RD/NI/LS/RO/RF/NP/OS/GC/VN
10	RC4/MR/HD	RC4/MR/HD/RD/NI/LS/RO/RF/NP/OS/GC/VN
11	RC5/MR/PD	RC5/MR/PD/RD/NI/LS/RO/RF/NP/OS/GC/VN

298 In relation to the seismic design levels, each building is modeled as indicated by the GLOSI taxonomy
299 as follows. Poor design (PD) buildings are only dimensioned to withstand gravity loads so they have
300 a very small capacity for lateral loads (no confinement stirrups). Low design (LD) buildings are
301 designed for low lateral loads, so no seismic confinement stirrups exist in the plastic hinge zone of
302 the elements (spacing between stirrups greater than $d/2$, where d is the distance from the extreme
303 compression fiber of the section to the centroid of the reinforcement). The minimum dimension of
304 structural elements at this design level is 200 mm. Fragile collapse mechanism and low lateral
305 capacity are expected for this case. Finally, high design (HD) buildings are designed for a high seismic
306 hazard zone with specific requirements as continuity in the longitudinal reinforcement of the
307 elements, confinement zone with a separation of stirrups equal to $d/4$ and the minimum dimension
308 for structural elements as 300 mm. The assumptions for each design level are based on the ASCE 7-
309 10 (ASCE and SEI 2017a) and the ACI 318-14 (ACI 2014) but adapted with expert criteria for a more
310 global application. Medium design was not considered in this study case since it differs considerably
311 between countries and design codes. Non-structural elements are designed to withstand seismic forces
312 unless specify otherwise. For this condition, it is expected ductile collapse mechanisms and very high
313 lateral capacity.

314

315 3.2 Ground motions

316 Once the IBs have been characterized, the next step is the hazard definition for the non-linear static
317 analysis. In this study, the possible hazard was based on an approach given by FEMA P-695 (ATC
318 2009). This approach considers a set of pre-selected, far-field and near-field real ground motions. In
319 the present application far-field records are used to assess more globally applicable characteristics.
320 This set has a PGA between 0.22 and 1.43g; a PGV between 30 and 167 cm/sec; a distance from the
321 source between 1.7 and 8.8 km; a minimum M_w of 6.5 and is selected for soft rock and stiff soil
322 conditions – e.g. soil types similar to NEHRP C & D (Building Seismic Safety Council 2003). The
323 acceleration spectrums for this set are presented in Fig. 4. However, additional sets such as near-field
324 or locally specific set can be used in other case studies. Given the global level application, no specific
325 additional consideration to the type of soil is included in the present application. However, the results
326 of a sensitivity analysis are discussed in section 4.2 to evaluate the effect of soil stiffness on the
327 capacity curves obtained for two different types of foundation configuration, and the resulting
328 vulnerability functions.



329

330 **Fig. 4** Far-field ground motion response spectra

331

332 **3.3 Structural modeling**

333 Details of the modelling considerations, material properties and general geometry details are
 334 presented in Table 2. These are based on information gathered from different countries, as
 335 documented in the GLOSI library (The World Bank 2019) and the recommendations given by the
 336 ASCE 41-17 (ASCE and SEI 2017b) for the non-linear analysis of RC buildings. The general
 337 geometric configuration is maintained in all IBs for consistency in the results. However, it is
 338 important to note that different buildings in reality may have slight variations in geometry, but this is
 339 out of the scope of this paper.

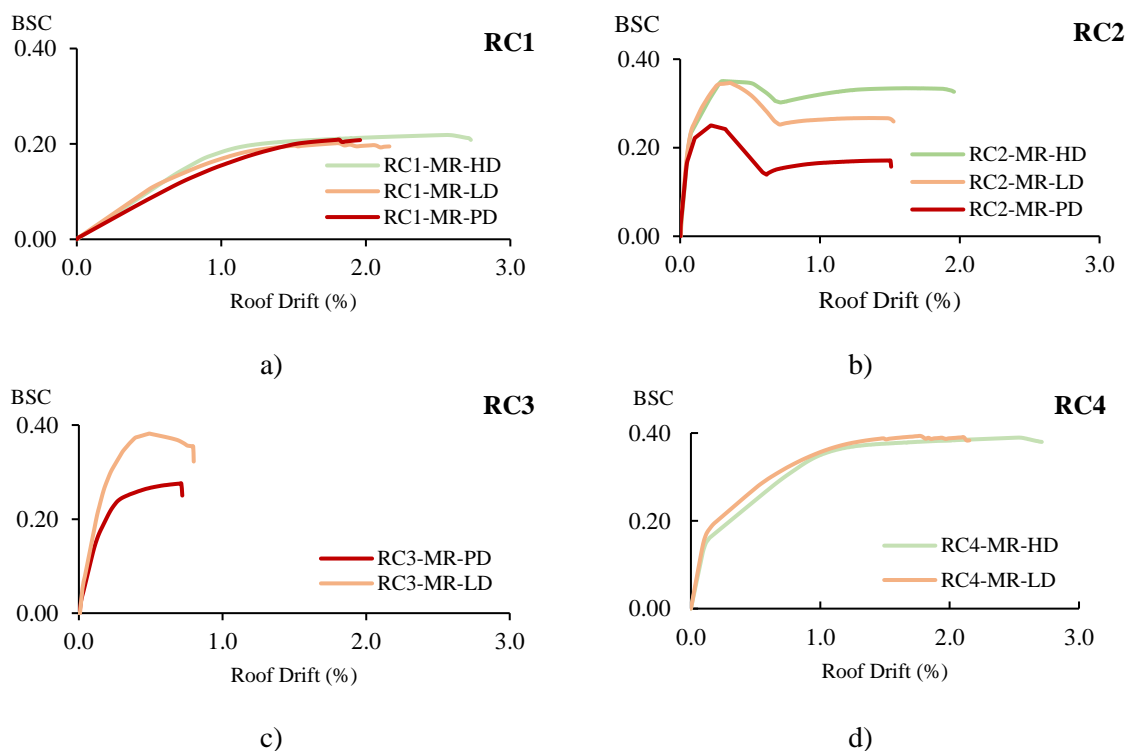
340 **Table 2** Modeling considerations

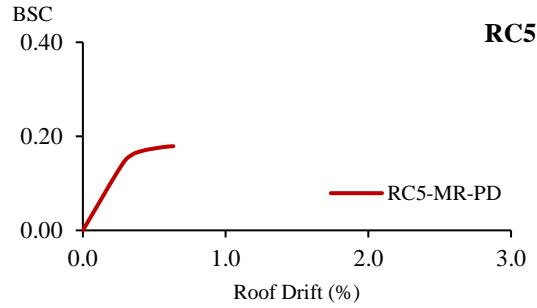
General considerations	Model type	3-D
	Non-linearity considerations	Concentrated plasticity (hinges) based on ASCE 41-17 (ASCE and SEI 2017b)
	Structural elements modeling strategy	Concrete beams and columns as frames, masonry infills modeled as equivalent struts and steel bracing as diagonal elements only considering its tensile capacity.
	P-Delta effects	Yes
	Rigid zones in nodes	Yes
	Rigid diaphragms	Floors and roof
	Cracked sections	Main structural elements
Loads considered in the analysis	Foundation flexibility	fixed based condition is adopted
	Elements self-weight	Yes
	Additional dead loads	Slabs, nonstructural walls, non-structural elements, roofs, ceilings, etc.
Material properties	Live load	25% of the design live load is considered for the non-linear analysis
	Concrete f'_c	PD: 17 Mpa; LD and HD: 21 Mpa
	Reinforcement f_y	PD, LD and HD: 420 MPa
Geometry	Masonry f'_m	2.8 Mpa
	Building plane area	300 m ²
	Story height	3 m
	Number of spans in long direction	7
	Typical span length in long direction	4.5 m
	Number of spans in short direction	3
	Typical span length in short direction	3.5 m
	Typical column dimensions (cm x cm)	Poor design:20 × 20; Low design:25 × 30; High design: 40 × 30
Typical beam dimensions (cm x cm)	Poor design:20 × 30; Low design:25 × 30; High design: 30 × 35	

341

342 Including the above considerations, the buildings were modeled using Perform3D software (CSI
 343 Computer & Structures Inc 2016), chosen because it provides enough reliability in the non-linear
 344 pushover analysis and allows to also run dynamic nonlinear analysis, which is also the basis for the
 345 sensitivity analysis and the validation approve. Moreover, Perform3D being a commercial software,
 346 it demonstrates that the methodology can be used by professionals as well as researchers.

347 Fig. 5 presents the pushover analysis for each typology and each design level. These results show that
 348 the main structural system defines the pushover curve with substantial differences between the main
 349 typologies, which confirm the suitability of the main classification. On the other hand, the parameter
 350 design level controls the maximum strength and the ductility capacity, also clearly indicating that the
 351 construction characteristics modifiers used to determine the design levels are appropriate to determine
 352 the capacity. Indeed, the RC2 and RC3 IBs have different pushover progressive structural behavior,
 353 but for both typologies, the resulting curves have different strength and ductility depending on the
 354 design level and the effect of the masonry infills interaction. Fig. 5 also shows that the RC1 and RC4
 355 typologies present similar pushover curves in shape, but with better structural behavior in RC4 in
 356 terms of initial stiffness and ultimate strength, while the ductility is preserved. The latter occurs since,
 357 in this case, the steel bracing was designed to fail at the drift level corresponding to the ultimate limit
 358 state of the concrete frames. However, other collapse sequences can be achieved when bigger or
 359 smaller sections of steel bracing are considered, which should be designed depending on the specific
 360 building code requirements of each case study. Finally, RC5 presents the lowest ductility and strength
 361 of a non-engineered structural system with low construction quality. It is also important to note that
 362 these results are obtained for fixed characteristic of geometry and design level, therefore results are
 363 significant for comparative purposes between typologies, but they do not capture the full range of
 364 behavior within a typology. To understand the effects of changes of the reference conditions chosen
 365 in this initial assessment, a sensitivity analysis varying the IB identifier parameters is presented in
 366 section 4. Also, damage state thresholds are not included in the pushover since the vulnerability
 367 derivation is component-based, and therefore, each component will have its own threshold.





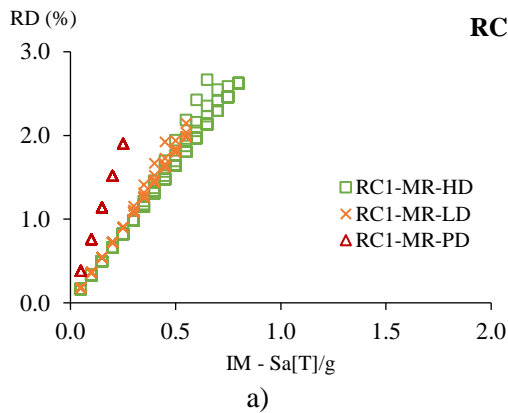
e)

368 **Fig. 5** Pushover curves (BSC = Base Shear Coefficient)

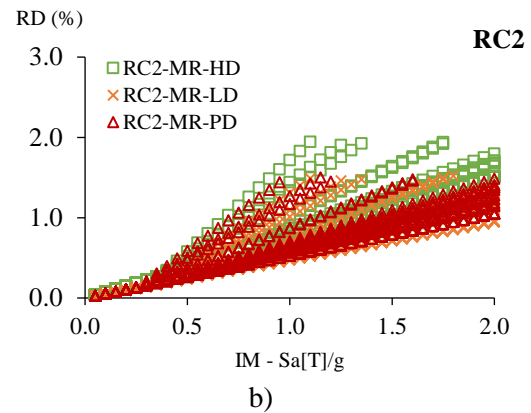
369

370 *3.4 Incremental static analysis*

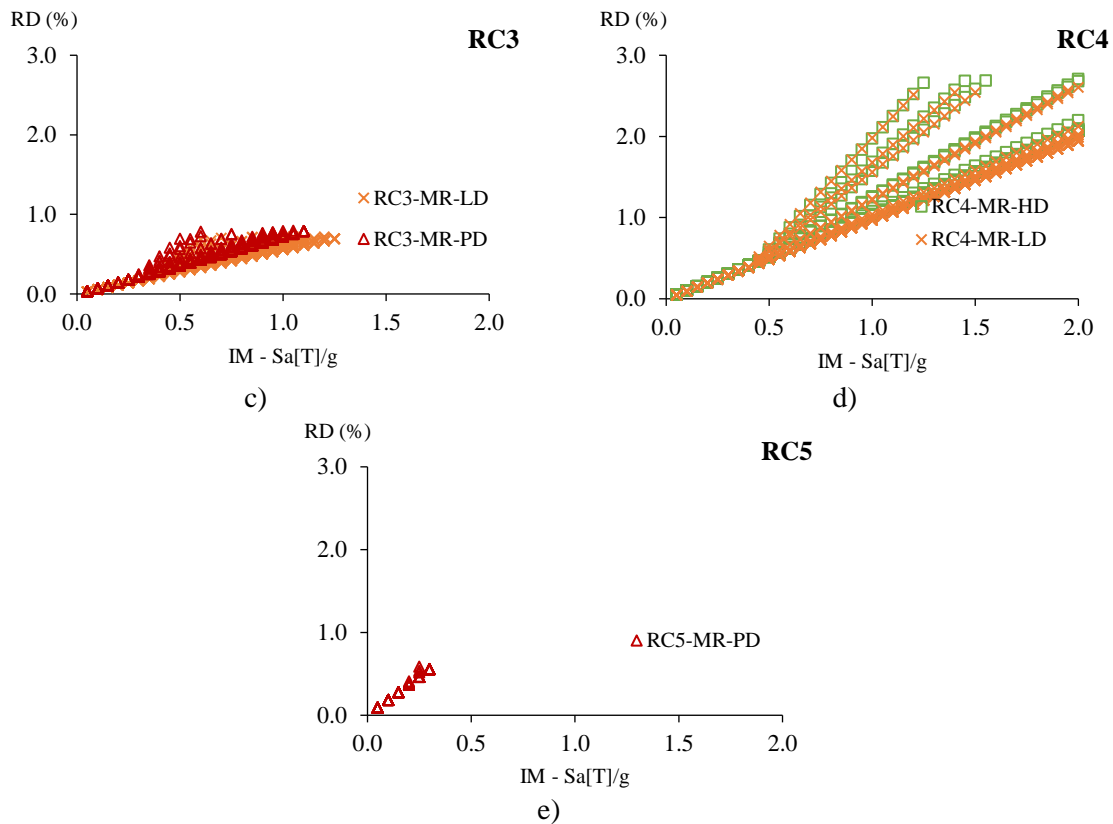
371 The integration of the hazard and the structural modeling is done by performing an incremental static
 372 analysis (ISA) based on the N2 method. This procedure results in the estimation of the engineering
 373 demand parameters (EDPs). These parameters were obtained by identifying the performance point,
 374 i.e., the intersection between the linearized pushover capacity curves shown in Fig. 5 and the non-
 375 linear response spectrum for each ground motion at each scaling stage. Further details of this
 376 methodology are explained in D’Ayala et al (2015). In this study, the analysis was developed to obtain
 377 the displacement for the roof and story level, as Engineering Demand Parameter (EDP). With these
 378 results, the roof drift and inter story drift are calculated using the story height. Fig. 6 presents the EDP
 379 results in terms of the roof drift for each structural system and each design level. These results show
 380 that the main structural system controls the structural behavior (as observed in the pushover analysis).
 381 The resulting EDPs are used to correlate with the damage state thresholds for each component
 382 included in the building, as presented in the following section.



a)



b)



383 **Fig. 6** RC mid-rise buildings engineering demand parameters – EDP (RD = Roof Drift)

384

385 3.5 Component and costs model

386 With the EDPs characterized for each building, the next step is the development of the component-
 387 and repair cost-based loss model, where estimated damage is expressed as repair/reconstruction vs.
 388 total cost. For this purpose, a component model, including structural and nonstructural elements, is
 389 assembled for each building under consideration, based on the FEMA P-58 vulnerable elements
 390 fragilities (ATC 2012). These set of fragilities were adapted for this specific case study to prove the
 391 global applicability of the proposed methodology by modifying the repair cost of each damage state
 392 to represent the conditions for low- or middle-income country based on previous studies in Latin
 393 America and the Caribbean (The World Bank 2018, 2020). However, further studies should be done
 394 to characterize the behavior of typical components for particular regions considering the local
 395 construction industry and details of the school infrastructure portfolio. The model includes all
 396 structural and non-structural components typical of school buildings, for each story. For each type of
 397 component, the measurement unit, the quantity of elements, fragility in terms of repair cost and time
 398 at different damage states, the controlling EDP, and correlation of damage between similar
 399 components at the same story is defined. Table 3 illustrates the typical component model for the
 400 buildings under consideration in this case study. The component model chosen depends on the
 401 architecture and construction characteristics as well as the context, region, or countries of which the
 402 IBs are representative. Therefore, for specific applications of this methodology the component model

403 in Table 3 will need tailoring. To understand how this affects the resulting vulnerability function, a
 404 sensitivity analysis is performed in section 4.

405 **Table 3** Component Model

Group	Description	Unit	Fragility specification code (FEMA P-58)	EDP	DS correlation between components	Structural typology
Structural	Columns and beam end nodes	Node	B1041.001a	Drift	No	All
Structural	Column and beam central nodes	Node	B1041.001b	Drift	No	All
Non-structural	Confined masonry facade	5mx3m	C1011.006b	Drift	Yes	All
Non-structural	Confined masonry partition wall (vener)	5mx3m	C1011.005b	Drift	Yes	RC2 and RC3
Non-structural	Confined masonry ¹ partition wall	5mx3m	C1011.004b	Drift	Yes	RC2 and RC3
Non-structural	Plastered ceiling	5mx5m	C3032.005a	Drift	No	All
Non-structural	Gas piping	22ml	D2022.025a	Drift	Yes	All
Non-structural	Electrical piping	110ml	D2021.011a	Drift	Yes	All
Non-structural	Water piping	62ml	D2022.011a	Drift	Yes	All
Contents	Contents (acceleration controlled)	5mx5m	E2022.010	Drift	No	All
Contents	Contents (drift controlled)	5mx5m	E2022.010a	Drift	No	All

406 Fragility functions were assigned to each component type in the model described above. They
 407 represent the probability of being in each damage state (usually slight, moderate, or extensive) as a
 408 function of the corresponding EDP (as defined previously). Each damage state is assigned a
 409 probability density function of repair cost and time, according to the FEMA P-58 (ATC 2012)
 410 catalogue. Further detail is given in Yamin et al (2017).

411

412 3.6 Vulnerability functions results and discussion

413 As described above, the integration of the previous results using a component-based method results
 414 in each IB's vulnerability function, which is the main result of the proposed methodology. The
 415 procedure to integrate the losses of each component in each EDP is described in Yamin et al (2017),
 416 which apply equally in this case, with the difference that the EDPs are obtained from an incremental
 417 static analysis instead of an incremental dynamic analysis. The vulnerability functions can be
 418 formulated using a beta distribution following Equation 1 (ATC 1985).

¹ Confined masonry refers to infill walls built with a secondary system of columns and beams ties in a framed RC building.

$$E[\beta] = E \left[1 - K \frac{V^\rho}{\gamma} \right] \quad (1)$$

419 where $E[\beta]$ is the expected MDR, V is the IM, K is the known MDR, γ the intensity for the known
 420 MDR K and ρ is the curvature parameter. The summary of the parameters for each function is
 421 presented in Table 4. The graphic results are presented in Fig. 7 (continuous line refers to the Mean
 422 Damage Ratio while the dotted line refers to the Variance in the results, this applies to all vulnerability
 423 functions presented herein).

424 **Table 4** Vulnerability functions parameters

Structural system	Height range	Seismic design level	Intensity at which damage begins	Intensity for complete damage	Inflection point Mean Damage Ratio (K)	Inflection point Intensity (γ)	Curvature before inflection point (ρ)	Curvature after inflection point (ρ)
RC1	Mid rise	Poor	0.08	0.30	50.00	0.20	5.00	5.00
		Low	0.10	1.10	50.00	0.55	2.30	3.00
		High	0.10	1.50	45.00	0.70	2.50	3.00
RC2	Mid rise	Poor	0.10	5.00	50.00	2.00	2.00	2.00
		Low	0.10	5.00	45.00	2.00	2.00	2.00
		High	0.10	5.00	40.00	2.00	2.00	2.00
RC3	Mid rise	Poor	0.10	5.00	50.00	1.00	3.00	4.00
		Low	0.10	5.00	50.00	1.10	4.00	5.00
RC4	Mid rise	Low	0.10	5.00	35.00	2.00	2.00	2.00
		High	0.10	5.00	25.00	2.00	2.00	2.00
RC5	Mid rise	Poor	0.10	0.60	50.00	0.35	3.50	4.00

425 The first set of vulnerability functions is presented in Fig. 7-a for the RC1 IB and each design level.
 426 The maximum Mean Damage Ratio (MDR) of 1.0 is reached for an IM of 0.4g, 1.0g and 1.5g for
 427 poor, low, and high design respectively. These results imply that this structural system may
 428 experience total collapse, even when the high design level is considered. These results also show a
 429 loss variance (indicated by the dotted line) of around 10% for each typology centered around a MDR
 430 of 0.25g, 0.6g and 0.8g for poor, low, and high design respectively.

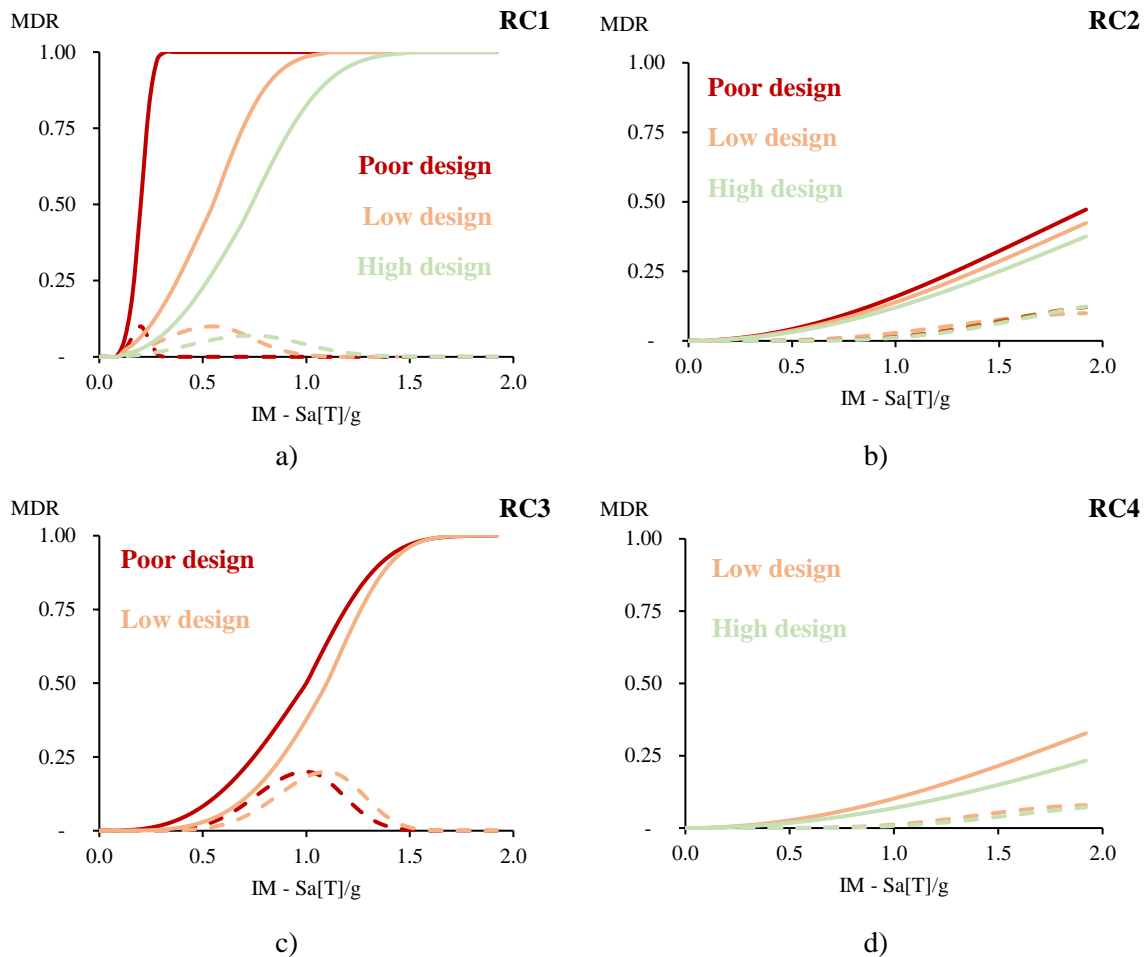
431 Fig. 7-b presents the second set of resulting vulnerability functions, showing the different design
 432 levels for the RC2 structural system. In contrast to the results obtained above, RC2 building
 433 typologies do not reach an MDR of 1.0 before a spectral acceleration of 2.0 g. These results indicate
 434 that this typology is less likely to collapse than RC1, however, it is important to note that variance in
 435 this range is usually larger than the one at the lower and larges IMs. Another change with respect to
 436 the previous results is that differences between design levels is not as noticeable as before, which is
 437 consistent with the resulting EDPs presented in Fig. 6. These minor differences suggest that in an
 438 RC2 typology, the design level does not control the vulnerability since the infills response governs
 439 the interaction between masonry walls and structural members.

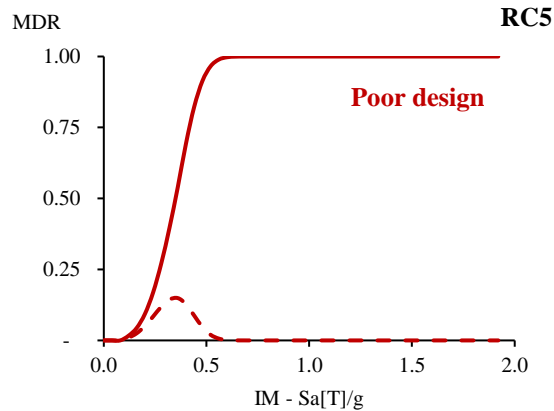
440 Fig. 7-c presents the results for the RC3 typology for poor and low design. These results show that
 441 this structural system presents a higher vulnerability to collapse (MDR = 1) than RC2 for intensity
 442 measures of about 1.5 g. This vulnerability condition is similar for both design levels, suggesting that
 443 the short column collapse mechanism controls the structural behavior. This conclusion is similar to

444 the one obtained before, which shows the high impact of the masonry infills in determining the
445 structural behavior of a school building.

446 Fig. 7-d shows the resulting vulnerability functions for the RC4 typology for low and high design
447 levels. These results indicate a low vulnerability in general for this typology, which is usually well
448 built and designed. The resulting vulnerability functions also suggests that this typology can be used
449 as a retrofitting option for the above IBs, reducing the MDR from 100% (total collapse) to only 25%.

450 Finally, as demonstrated in Fig. 7-e, the RC5 structural systems have a high vulnerability, presenting
451 collapse for intensity measures around 0.5 g. This level is only comparable with the vulnerability
452 presented for RC1 poor design level buildings, which is also a highly vulnerable typology.





e)

453 **Fig. 7** RC mid-rise buildings vulnerability functions (MDR = Mean Damage Ratio)

454 The vulnerability functions presented above are compared directly for illustration purposes. However,
 455 it is essential to note that two similar curves of different IBs can lead to different risk results when
 456 integrating hazard and exposure. This difference occurs because different typologies may have
 457 different structural periods, resulting in a different hazard level (IM) and, hence, a different level of
 458 damage. This type of analysis is out of the scope of the present study but should be conducted for
 459 understanding the risk results at a regional level and for the development of effective retrofitting
 460 programs.

461

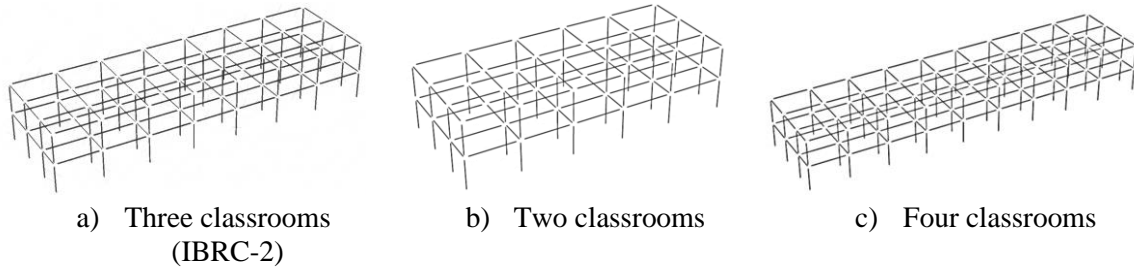
462 **4 Sensitivity analysis**

463 Different construction characteristics in a portfolio of buildings represented by one IB pose a number
 464 of uncertainties, from actual material properties of masonry components to variation in geometry and
 465 layout. Also, the consideration of non-structural elements and the modelling strategy affects the final
 466 vulnerability functions of IBs. To analyze this uncertainty, a sensitivity analysis is performed,
 467 including variations in five different parameters. The first one is geometry, which is included since
 468 there is high variation between countries and inside each country. For example, buildings usually
 469 include three classrooms, but in smaller schools there exists submodules of two or even one
 470 classroom, while in larger school facilities modules of four or five classrooms can be found. The
 471 second parameter is the foundation-soil flexibility, which is included mainly due to the spatial
 472 variability, and therefore uncertainty, of the soil conditions. The third parameter is the quality of
 473 masonry infills, that varies among countries. For example, in El Salvador and the Dominican
 474 Republic, it is very common to find infill walls of reinforced concrete blocks while in Colombia such
 475 walls are unreinforced clay bricks. The fourth parameter analyzed is the effect of including the losses
 476 associated with non-structural vulnerable elements. Finally, the analysis type is also considered since
 477 it can have an important influence on the results. These analysis are done independently following
 478 the One Factor at a Time (OFT) method (Porter et al. 2002).

479

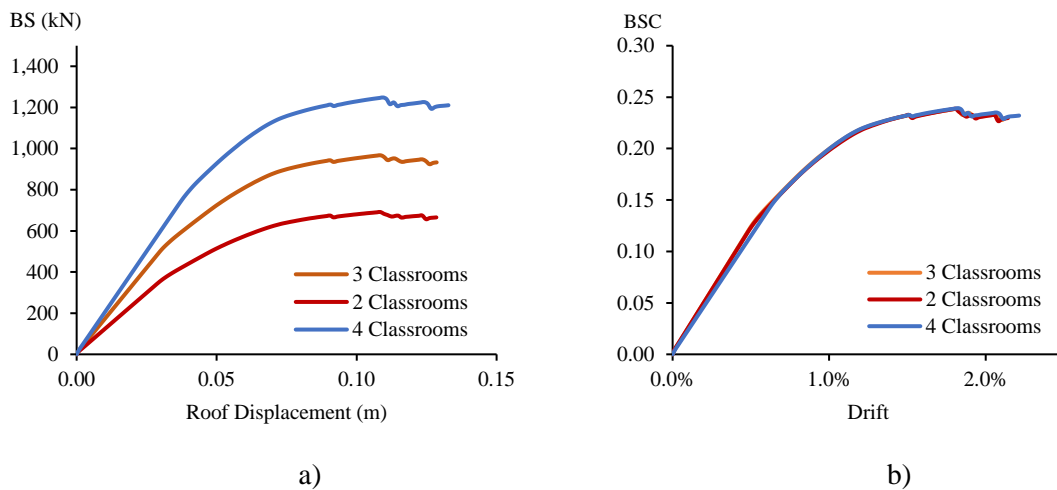
480 4.1 Geometrical variations

481 To understand how geometrical variations of the school buildings layouts affect the vulnerability
 482 functions, an RC1 mid-rise building with low seismic design (RC1/MR/LD) was analyzed. Three
 483 different layouts were selected for the analysis as illustrated in Fig. 8, representing a plan with three
 484 (the most common), two and four typical classrooms. All models are two-story buildings, and the
 485 frame dimensions and reinforcement details are maintained constant.



486 **Fig. 8** School buildings modules

487 Fig. 9 presents the capacity curves relating the maximum roof displacement associated to different
 488 total base shear forces. Normalized pushover curves for the three models, shown in Figure 13b in
 489 terms of the Base Shear Coefficient (BSC), do not present significant variations. Considering that the
 490 Engineering Demand Parameters (EDPs) are obtained using the N2 method, no significant variations
 491 are expected in the final vulnerability functions for the three models. Therefore, it is concluded that
 492 the vulnerability function for the three-classroom model is representative of other general plan
 493 layouts, as long as no irregularities or other critical structural behavior is generated with alternative
 494 layouts.



495 **Fig. 9** Capacity curves for different geometries (BS = Base Shear, BSC = Base Shear Coefficient). a)
 496 Capacity curves. b) Normalized capacity curves

497

498 4.2 Foundation-soil flexibility

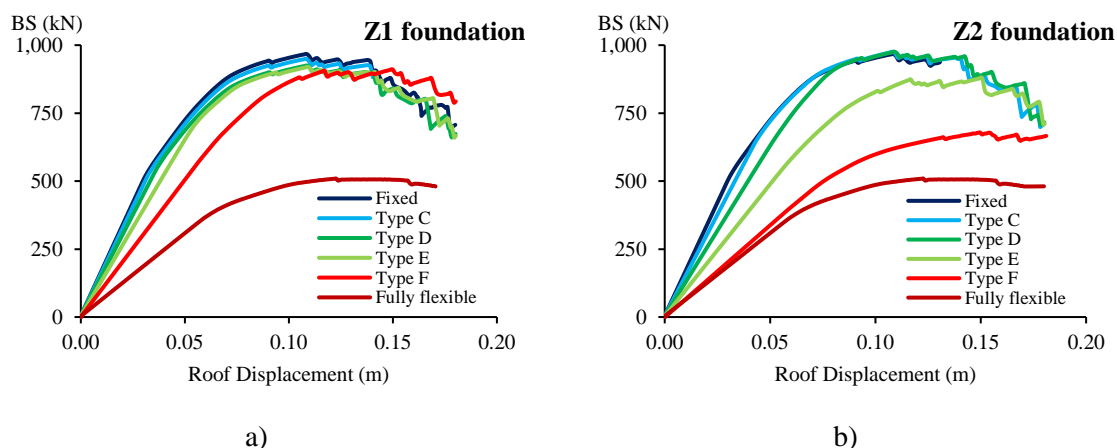
499 To assess the possible variations in the vulnerability functions for different soil-foundation stiffness,
 500 the RC1 mid-rise building with low seismic design (RC1/MR/LD) was analyzed using two different

501 foundation configurations: 1.0 m by 1.0 m (Z1) and a 0.5 m by 0.5 m. (Z2) isolated footings. Each of
 502 these configurations was combined with four different soil types as indicated in Table 5 (Wald and
 503 Allen 2007; ASCE and SEI 2017a). Resulting capacity curves are presented in Fig. 10 for all possible
 504 combinations of foundation and soil type. Corresponding vulnerability functions are presented in Fig.
 505 11, including the results for the full rigid and full flexible cases which are the same for both Z1 and
 506 Z2 configurations.

507 **Table 5** Soil properties for foundation stiffness calculation

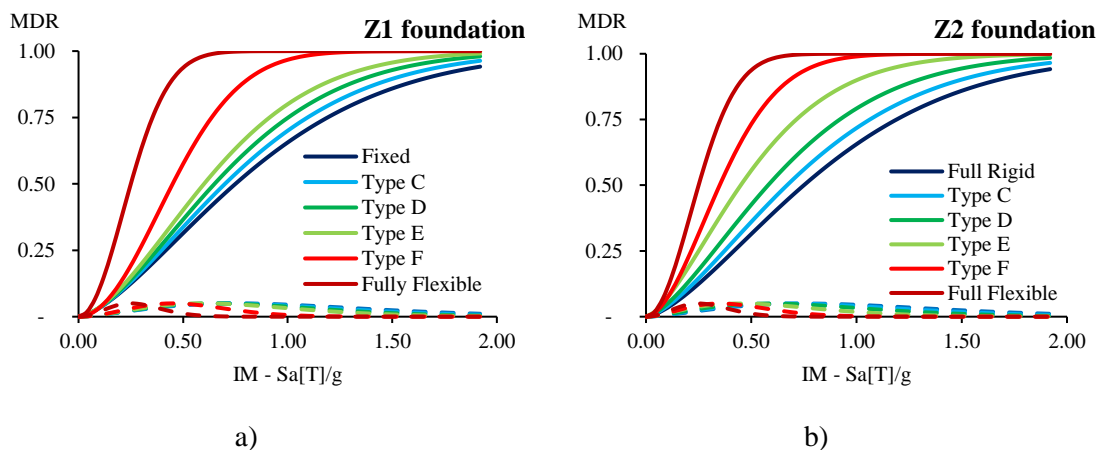
Type	G/G_0	Soil Type	Density _{sat} (kN/m ³)	Mean V_{s30} (m/s ²)	ν
C	0.9	Lime	22	500	0.35
D	0.81	Clay	18	300	
E	0.47	Clay	18	200	
F	0.32	Clay	18	100	

508



509 **Fig. 10** Capacity curves with foundation in different soil types (BS = Base Shear)

510



511 **Fig. 11** Vulnerability functions with different foundation stiffness (MDR = Mean Damage Ratio)

512 From the results it is possible to conclude that good foundation configurations (represented by Z1
 513 footings) will generate pushover curves and vulnerability functions showing a behavior closer to the

514 rigid base model assumption, showing an IM of around 0.7 g for the fix-end assumption to 0.56 g for
 515 the Type E soil for 50% MDR. However, for a considerable flexible soil (type F), the vulnerability is
 516 substantially increased, presenting an IM of 0.44 g for 50% of damage and total damage at an IM of
 517 1.00 g. For relatively weak foundation configurations (represented by Z2 footings), higher
 518 vulnerability curves are obtained with considerable variations for different soil types. For stiff soil
 519 profiles (soil types C or D in the previous table) the expected behavior will approximate the fixed
 520 base assumption. On the other hand, for flexible soil profiles (soil types E, or F) the expected behavior
 521 will approximate the hinged base assumption. It is important to note that this combination may not
 522 be found in reality but it is included in the analysis as an illustrative case for comparison. In
 523 conclusion, the most common assumption of rigid base behavior can be sustained only when a
 524 relatively good foundation configuration is expected in medium or stiff soil profiles. In the cases
 525 where there is evidence of soft soil profiles with probable deficiencies in the foundation configuration,
 526 flexible support conditions shall be considered in the assessment, given that those conditions will
 527 generate a higher vulnerability for the building under consideration.

528

529 4.3 Masonry infills quality

530 To test the relevance of masonry infills quality in the resulting vulnerability function, different
 531 masonry properties were selected, additional to the ones selected in section 3, as summarized in Table
 532 6. These masonry properties were selected by the authors based on the test developed by Carrillo
 533 (2004) and with new materials available for construction in Colombia. In this case, the variations in
 534 masonry were analyzed in the IB model RC2, mid-rise building with low seismic design
 535 (RC2/MR/LD), for which infill are explicitly modelled to quantify their contribution to structural
 536 response.

537 **Table 6** Masonry properties

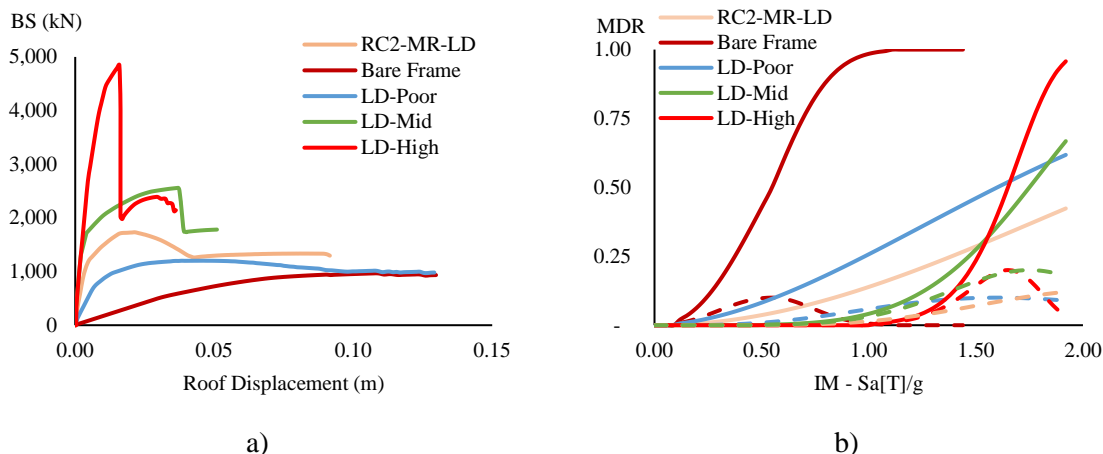
Quality	Block Material	Dimensions (bxlxt)	f_v (Mpa) ²	f'_m (Mpa) ³	Friction coefficient
High	Clay brick	10x20x6	0.9	12	0.7
Medium	Clay brick	10x28x6	0.1	4.7	
Poor	Clay tile	11x30x20	0.1	2.0	
Reference	Clay brick	10x20x6	0.6	2.8	

538 Fig. 12a presents the capacity curves for the three assumptions of masonry quality as compared to the
 539 bare frame (no masonry infills) conditions and the reference IB (RC2-MR-LD). From the figure, it is
 540 clear that masonry infills, when not isolated from the structure, can heavily affect the expected
 541 structural behavior of the building. Also, the collapse mechanism of the building can significantly
 542 change, as more resistant but fragile behavior can be obtained. For the cases of High, Medium and
 543 Reference quality infills, weak floor failure mechanism can be generated when the ground-floor infill
 544 walls fail under horizontal seismic loading.

² f_v = cohesion

³ f'_m = compressive strength of the masonry wall

545 Fig. 12b shows the great variability in the results expected for the range of masonry infills qualities
 546 considered. It is worth noting that the curves are not directly comparable because the building
 547 structural predominant period (T_1) will significantly change depending on the quality of the masonry
 548 infills and therefore different intensity parameter will be used for the risk assessment (for direct
 549 comparison between the vulnerability functions, they should be transformed –or derived from the
 550 beginning– for PGA or another equivalent IMs for all functions). In conclusion, the quality of the
 551 masonry infills in a school building (if not isolated from the main structure) will have a significant
 552 impact in the final vulnerability of the building. Therefore, it is highly recommended to consider the
 553 quality of the masonry infills as a critical variable for the assessment.



554 **Fig. 12** a) capacity curves using different masonry qualities (BS = Base Shear). b) vulnerability functions
 555 using different masonry qualities (MDR = Mean Damage Ratio).

556

557 **4.4 Non-structural vulnerable elements**

558 The objective of this sensitivity analysis is to identify the effect of considering different types of non-
 559 structural elements (NSE) in the loss calculation process. For this, mid-rise RC1 IB with high seismic
 560 design level (RC1/MR/HD) is selected since masonry walls do not interact directly with the reinforced
 561 concrete frames, which as showed in the previous section, highly affects the results. The following
 562 three conditions are considered: (i) no consideration of non-structural elements, (ii) poor quality
 563 fragile non-structural elements and (iii) high quality ductile non-structural elements. Table 7 to Table
 564 9 present the component models for these three conditions. It is important to clarify that the non-
 565 structural elements for façade and internal partitions walls, presented in Table 8 and Table 9, are
 566 isolated from the structure and therefore does not affect the structural behavior of the RC moment
 567 resistant frames (RC1).

568 **Table 7** Only structural elements component model

Group	Description	Quantity	Fragility specification code	EDP
Structural	Column-one beam	8	B1041.091a	Drift
Structural	Column-two beams	21	B1041.091b	Drift

569

570 **Table 8** Poor quality component model

Group	Description	Quantity	Fragility specification code	EDP
Structural	Column-one beam	8	B1041.091a	Drift
Structural	Column-two beams	21	B1041.091b	Drift
Non-structural	Unreinforced Masonry (URM) facade	14	C1011.006a	Drift
Non-structural	URM wall	6	C1011.006b	Drift
Contents	Contents	13	E2022.010a	Drift

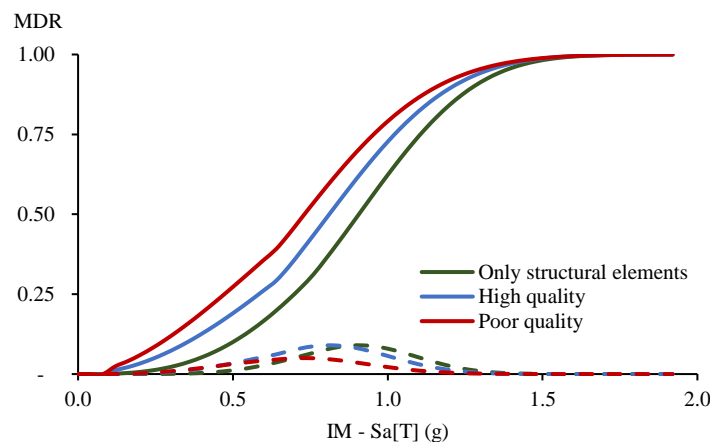
571

572 **Table 9** High quality component model

Group	Description	Quantity	Fragility specification code	EDP
Structural	Column-one beam	8	B1041.001a	Drift
Structural	Column-two beams	21	B1041.001b	Drift
Non-structural	Confined masonry (CM) facade	14	C1011.001a	Drift
Non-structural	CM wall	6	C1011.001a	Drift
Contents	Contents	13	E2022.010a	Drift

573

574 Fig. 13 presents the vulnerability curves for each one of the cases explained above. From these results
 575 it can be concluded that variations on the order of 20% in the mean damage ratio could be expected
 576 when considering fragile NSE as compared with a building with no NSE for the lower ranges of
 577 seismic intensities. In addition, lower relative variations are expected in the higher range of seismic
 578 intensities, since global building collapses would control the losses in that intensity range.



579

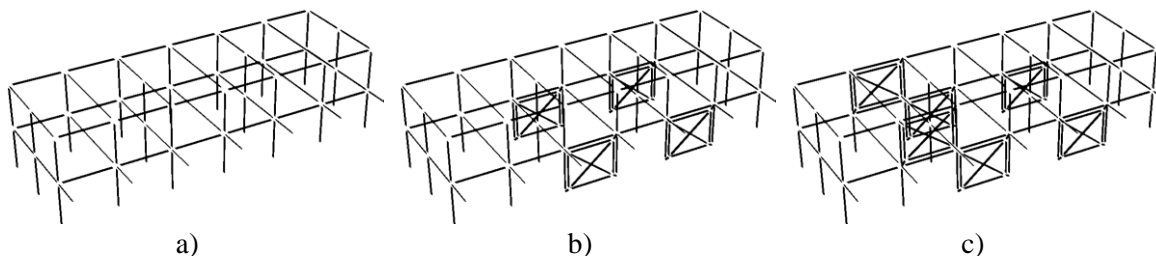
580 **Fig. 13** Vulnerability functions using different component models (MDR = Mean Damage Ratio)

581 As a general recommendation, NSE shall be included in the vulnerability assessment when they
 582 represent a significant replacement value as compared to the structure itself, and when they present
 583 fragile behavior and significant damage during an earthquake (no seismic design). The consideration
 584 of the NSE in those cases will generate a significant increase in the mean damage ratio of the global
 585 building especially for the low range of seismic intensities and will therefore affect significantly the
 586 expected annual losses in the risk assessment process.

588 4.5 Analysis type

589 To establish the reliability of using the non-linear static N2 method, finally a comparison is carried
 590 out with results obtained by applying incremental dynamic analysis (IDA) approach to an IB without
 591 and with retrofitting. Literature highlighting non negligible differences between the nonlinear
 592 dynamic methods and nonlinear static procedures usually focuses on high rise buildings, whereby
 593 upper modes have greater contribution (Han and Chopra 2006; Reyes and Chopra 2011). However,
 594 the proposed methodology focuses on low and mid-rise school buildings, usually regular in height
 595 and floor plan. Available calibrations and results for these types of buildings show good correlation
 596 between the simplified methodology and more complex procedures like incremental dynamic analysis
 597 (Mwafy and Elnashai 2001; Dolšek and Fajfar 2004, 2008; Faella et al. 2008; Bhatt and Bento 2011;
 598 Causevic and Mitrovic 2011; Gehl et al. 2014; Rossetto et al. 2014). As an additional comparison for
 599 validation purposes, results from both incremental dynamic analysis (IDA) –obtained through a non-
 600 linear time history analysis using the commercial software Perform3D with the modelling
 601 considerations presented in Table 2– and the incremental static analysis (ISA) proposed in this
 602 methodology are compared. Fig. 14 presents the three selected buildings models, which are based on
 603 a common school typology found in Peru (Fernández et al. 2019). The Basic IB is a RC1, a mid-rise
 604 building with low design level (RC1-MR-LD). The second model is the same building with a
 605 retrofitting system of steel diagonals in the first story which shift is taxonomy to a RC4-MR-LD. The
 606 third model includes the retrofitting system at both stories obtaining a type RC4-MR-HD.

607

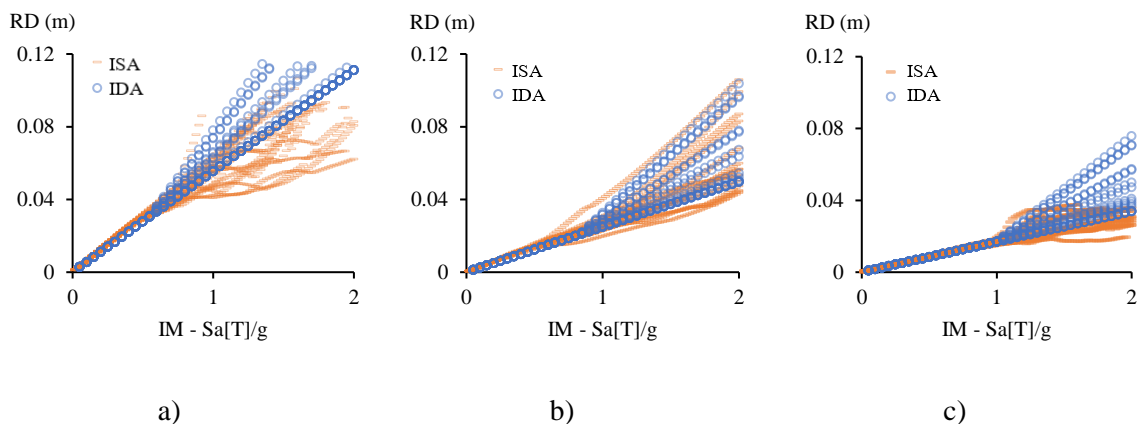


608 **Fig. 14** School buildings analyzed for the IDA vs. ISA comparison. a) RC1-MR-LD, b) RC4-MR-LD, and c)
 609 RC4-MR-HD

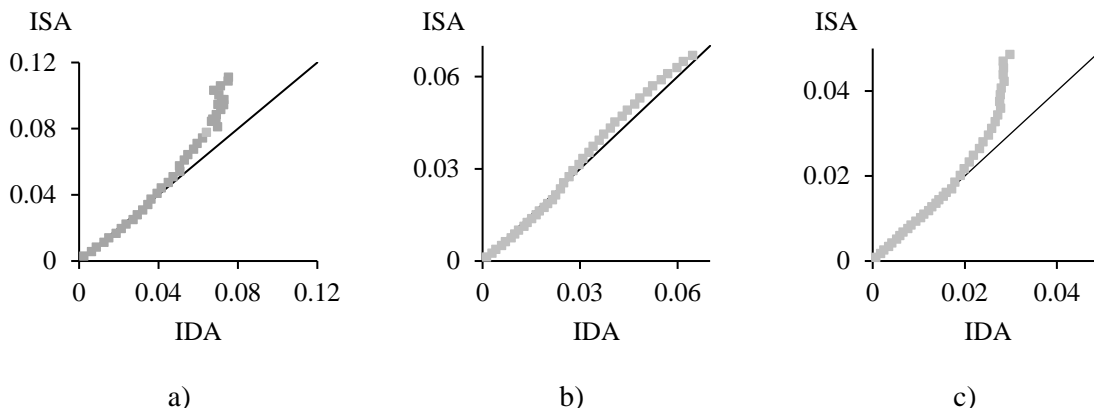
610 Fig. 15 shows the resulting Roof Drift (RD) obtained with ISA and IDA methodologies using the set
 611 of ground motions presented in section 3.2. The results show a high correlation between the mean
 612 roof drift found with IDA and ISA procedures. Results show that the maximum roof drift found in
 613 each building is similar for both methodologies. In addition to the above, Fig. 16 presents the mean
 614 RD obtained with each methodology for all three typologies. Based on these results, the mean square
 615 error (MSE) between ISA and IDA results in 0.016, 0.002, and 0.007 for RC1-MR-LD, RC4-MR-
 616 LD, and RC4-MR-HD, respectively. It is important to note that the MSE is very small for all the
 617 buildings, particularly for RC4-MR-LD. Additionally, the mean absolute percentage error (MAPE)
 618 between methodologies is about 19.1%, 8.4%, and 16.3% for RC1-MR-LD, RC4-MR-LD, and RC4-
 619 MR-HD, which is relatively low considering the simplification of the ISA methodologies. The
 620 obtained relative error may be explained on the simplifications of the ISA method, particularly with
 621 working with the resulting spectrum and not with the ground motion itself. This comparison suggests

622 that both methodologies yield similar results, despite being limited to the regular buildings analyzed
 623 herein. This type of results will not necessarily be obtained if the analyzed buildings are taller than
 624 three stories or have any irregularity. For these types of buildings, modifications of the N2 method
 625 have been proposed (Kreslin and Fajfar 2012; Magliulo et al. 2012), but are beyond the scope of the
 626 present study.

627



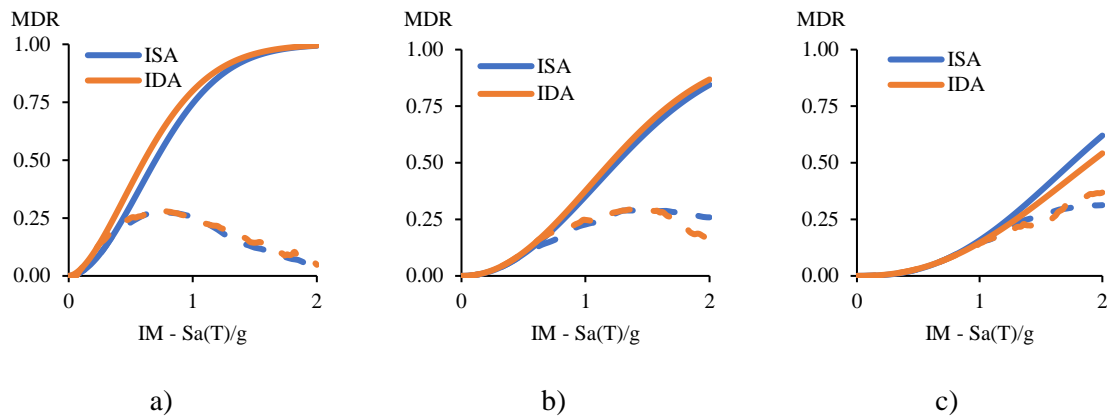
628 **Fig. 15** EDP using ISA and IDA methodologies (RD = Roof Displacement). a) RC1-MR-LD, b) RC4-MR-
 629 LD, and c) RC4-MR-HD



630 **Fig. 16** Mean Roof Drift (m) using IDA vs. ISA. a) RC1-MR-LD, b) RC4-MR-LD, and c) RC4-MR-HD

631 Fig. 17 presents the resulting vulnerability functions for the three buildings, using both
 632 methodologies. From these results it can be concluded that the N2 method, which in general is much
 633 simpler and faster to run, gives comparable results with the more refined and time-consuming IDA
 634 method of analysis. It is also important to note that the N2 method considers the non-linear behavior
 635 of buildings (hysteretic behavior, pinching and buckling of rebar among others) in a simplified way
 636 through the ductility and the pushover of the building. However, from the results it is possible to
 637 establish that both methodologies generate similar mean and dispersion values of the vulnerability
 638 function. For the vulnerability assessment of typical school buildings, the N2 method is clearly a
 639 reliable option to determine structural response. Caution shall be exerted when considering non-
 640 typical school buildings whose behavior is influenced by irregularities, variations in height, combined
 641 structural systems or any other special characteristic.

642



643 **Fig. 17** Vulnerability functions (MDR = Mean Damage Ratio): a) RC1-MR-LD, b) RC4-MR-LD, and c)
 644 RC4-MR-HD

645 5 Summary and conclusions

646 The present study shows how by classifying typical global RC school buildings according to their
 647 construction characteristics, and focusing on these when developing structural modelling, their
 648 specific structural system and their corresponding design level, their seismic response and
 649 vulnerability can be clearly characterized and quantified with good levels of confidence. As a first
 650 conclusion from the work presented in this study, the structural system is the main parameter affecting
 651 seismic response and hence, economic losses. As a matter of fact, typologies such as RC1, RC3 and
 652 RC5 can reach 100% of damage for low IMs (<1.5g), while RC2 and RC4 reach a maximum level of
 653 damage between 20 and 50% for a maximum IM of 2.0g. Another relevant result is that the
 654 vulnerability functions depend also on the design level, with a higher impact in this regard for the
 655 RC1 than in the RC2, RC3 and RC4. Indeed, the variation between design level for the RC1 IBs can
 656 increase until 80% for the same IM, while for RC2, RC3 and RC4 IBs it reaches a maximum value
 657 of 10% for the range of IMs analyzed. This impact can be explained by the infills high contribution
 658 in the final structural behavior of the entire system, even in ductile structures. Ductility also plays an
 659 important role in determining seismic response and vulnerability, as seen in the RC4 typologies and
 660 the RC1 high design IB. In general terms, since a higher vulnerability was identified for RC1, RC3,
 661 and RC5 compared to the results for RC2 and RC4, the former systems may be prioritized in a risk
 662 reduction retrofitting program, although this type of preliminary assessment for prioritization should
 663 weigh other factors as well, such as economic and technical viability, relative importance (e.g., terms
 664 of student demand), or other functional and operative considerations.

665 The proposed methodology provides an efficient and reliable procedure to assess the seismic
 666 vulnerability in school buildings and may be widely applied in different contexts for school
 667 infrastructure worldwide. In addition, the methodology explicitly quantifies the uncertainty
 668 associated with the vulnerability value, allowing for an unbiased and consistent strategy to assess the
 669 vulnerability of school buildings. This assessment is the first step to quantify the risk level of school
 670 infrastructure in a specific region and to develop a set of strategies with the aim of reducing
 671 vulnerability and protecting the students and all the community associated to school infrastructure.
 672 These vulnerability results can be used and helps for the developing intervention strategies at scale,
 673 such as the incremental retrofitting. As presented in section 3 the main parameters like structural

674 system, height and design level highly impacts the resulting vulnerability of buildings. However,
675 secondary parameters such as the infills type or the foundation also affects the vulnerability as showed
676 in section 4, and therefore should be considered as they directly impact the economic losses and costs.
677 Other factors such as variation in story height, vertical or horizontal irregularities were not considered
678 in this study and further analysis is needed to understand the full spectrum of vulnerability of other
679 type of RC school building.

680 **Acknowledgments**

681 This study was developed under the Global Program for Safer Schools (GPSS), funded by the Global
682 Facility for Disaster Reduction and Recovery (GFDRR) of The World Bank. The authors are thankful
683 to the World Bank and the entire GPSS technical team, and especially to its directors Fernando
684 Ramirez and Carina Fonseca. Gratitude is also extended to the Research Center on Materials and
685 Civil Infrastructure (CIMOC) from Universidad de Los Andes and the EPICentre from University
686 College London and all its members for the valuable work and feedback during the project. Finally,
687 this paper is dedicated to the memory of Prof. Dr. Luis E. Yamin, team leader of CIMOC at
688 Universidad de los Andes for over 30 years, who directed this research and considered it as his
689 personal priority.

690 **References**

691

- 692 Abo-El-ezz A, Nolle MJ, Nastev M (2013) Seismic fragility assessment of low-rise stone masonry
693 buildings. *J Earthq Eng Eng Vib* 12:87–97. <https://doi.org/10.1007/s11803-013-0154-4>
- 694 ACI (2014) Building Code Requirements for Structural Concrete (ACI 318-14). American Concrete
695 Institute, USA
- 696 Adhikari RK (2021) A Methodological Framework for Seismic Vulnerability Assessment of Masonry
697 School Buildings: Application to Nepal (Doctoral Dissertation). University College London
- 698 Aleskerov F, Say AI, Toker A, et al (2005) A cluster-based decision support system for estimating
699 earthquake damage and casualties. *Disasters* 29:255–276. <https://doi.org/10.1111/j.0361-3666.2005.00290.x>
- 701 ASCE, SEI (2017a) ASCE 7-16: Minimum design loads and associated criteria for buildings and
702 other structures. American Society of Civil Engineers
- 703 ASCE, SEI (2017b) ASCE/SEI 41-17: American Society of Civil Engineers, seismic evaluation and
704 retrofit of existing buildings. American Society of Civil Engineers
- 705 ATC (2009) FEMA P695: Quantification of building seismic performance factors. Applied
706 Technology Council, Redwood City, California
- 707 ATC (2005) FEMA 440: Improvement of Nonlinear Static Seismic Analysis Procedures. Applied
708 Technology Council, Redwood City, California
- 709 ATC (2012) FEMA P-58: Seismic Performance Assessment of Buildings. Applied Technology
710 Council, Redwood City, California
- 711 ATC (1985) Earthquake Damage Evaluation Data for California, ATC-13. Applied Technology
712 Council, Redwood City, California

713 Baker JW (2011) Conditional Mean Spectrum: Tool for Ground-Motion Selection. *J Struct Eng*
714 137:322–331. [https://doi.org/10.1061/\(asce\)st.1943-541x.0000215](https://doi.org/10.1061/(asce)st.1943-541x.0000215)

715 Bhatt C, Bento R (2011) Assessing the seismic response of existing RC buildings using the extended
716 N2 method. *Bull Earthq Eng* 9:1183–1201. <https://doi.org/10.1007/s10518-011-9252-8>

717 Building Seismic Safety Council (2003) FEMA 450: NEHRP Recommended Provisions for Seismic
718 Regulations for New Buildings and Other Structures. National Institute of Building Sciences,
719 Washington DC

720 Carrillo J (2004) Modelación del comportamiento inelástico de pórticos de concreto con mampostería
721 no reforzada. Universidad de los Andes

722 Causevic M, Mitrovic S (2011) Comparison between non-linear dynamic and static seismic analysis
723 of structures according to European and US provisions. *Bull Earthq Eng* 9:467–489.
724 <https://doi.org/10.1007/s10518-010-9199-1>

725 Chen H, Xie Q, Lan R, et al (2017) Seismic damage to schools subjected to Nepal earthquakes, 2015.
726 *Nat Hazards* 88:247–284. <https://doi.org/10.1007/s11069-017-2865-8>

727 Chopra AK, Goel RK (2002) A modal pushover analysis procedure for estimating seismic demands
728 for buildings. *Earthq Eng Struct Dyn* 31:561–582. <https://doi.org/10.1002/eqe.144>

729 Cremen G, Baker JW (2019) A methodology for evaluating component-level loss predictions of the
730 FEMA P-58 seismic performance assessment procedure. *Earthq Spectra* 55:193–210.
731 <https://doi.org/10.1193/031618EQS061M>

732 CSI Computer & Structures Inc (2016) PERFORM 3D - Performed-Based Design of 3D Structures

733 CSI Computer & Structures Inc (2020) ETABS - Building Analysis and Design

734 CSI Computer & Structures Inc (2004) SAP2000 - Linear and Nonlinear Static and Dynamic Analysis
735 of Three-Dimensional Structures

736 D’Ayala D (2013) Assessing the seismic vulnerability of masonry buildings. In: *Handbook of Seismic
737 Risk Analysis and Management of Civil Infrastructure Systems*. pp 334–365

738 D’Ayala D, Galasso C, Nassirpour A, et al (2020) Resilient communities through safer schools. *Int J
739 Disaster Risk Reduct* 45:101446. <https://doi.org/10.1016/j.ijdr.2019.101446>

740 D’Ayala D, Meslem A, Vamvatsikos D, et al (2015) Guidelines for Analytical Vulnerability
741 Assessment - Low/Mid-Rise. *GEM Tech Rep* 12:162. <https://doi.org/10.13117/GEM.VULN-MOD.TR2014.12>

742

743 Del Gaudio C, Ricci P, Verderame GM, Manfredi G (2015) Development and urban-scale application
744 of a simplified method for seismic fragility assessment of RC buildings. *Eng Struct* 91:40–57.
745 <https://doi.org/10.1016/j.engstruct.2015.01.031>

746 Di Trapani F, Shing PB, Cavaleri L (2018) Macroelement Model for In-Plane and Out-of-Plane
747 Responses of Masonry Infills in Frame Structures. *J Struct Eng* 144:04017198.
748 [https://doi.org/10.1061/\(asce\)st.1943-541x.0001926](https://doi.org/10.1061/(asce)st.1943-541x.0001926)

749 Digicon Engineering Consult, The World Bank (2016) Structural Integrity and Damage Assessment
750 (SIDA) for Educational Infrastructures in Nepal

751 Dolšek M (2012) Simplified method for seismic risk assessment of buildings with consideration of
752 aleatory and epistemic uncertainty. *Struct Infrastruct Eng* 8:939–953.

- 753 <https://doi.org/10.1080/15732479.2011.574813>
- 754 Dolšek M, Fajfar P (2005) Simplified non-linear seismic analysis of infilled reinforced concrete
755 frames. *Earthq Eng Struct Dyn* 34:49–66. <https://doi.org/10.1002/eqe.411>
- 756 Dolšek M, Fajfar P (2004) IN2 - A Simple alternative for IDA. In: 13th World Conference on
757 Earthquake Engineering. p 15
- 758 Dolšek M, Fajfar P (2008) The effect of masonry infills on the seismic response of a four-storey
759 reinforced concrete frame - a deterministic assessment. *Eng Struct* 30:1991–2001.
760 <https://doi.org/10.1016/j.engstruct.2008.01.001>
- 761 EERI (2019) *Concrete Buildings Damaged in Earthquakes*. Oakland, CA
- 762 Elwood KJ (2004) Modelling failures in existing reinforced concrete columns. *Can J Civ Eng* 31:846–
763 859. <https://doi.org/10.1139/L04-040>
- 764 European Committee for Standardization (2004) Eurocode 8: Design of structures for earthquake
765 resistance. CEN, EN 1998-1, Brussels
- 766 Ezzeldin M, Wiebe L, El-Dakhkhni W (2016) Seismic Collapse Risk Assessment of Reinforced
767 Masonry Walls with Boundary Elements Using the FEMA P695 Methodology. *J Struct Eng*
768 142:04016108. [https://doi.org/10.1061/\(asce\)st.1943-541x.0001579](https://doi.org/10.1061/(asce)st.1943-541x.0001579)
- 769 Faella C, Lima C, Martinelli E (2008) Non-linear Static Methods For Seismic Fragility Analysis and
770 Reliability Evaluation of Existing Structures. 14th World Conf Earthq Eng
- 771 Fajfar P (2000) A Nonlinear Analysis Method for Performance-Based Seismic Design. *Earthq Spectra*
772 16:573–592. <https://doi.org/10.1193/1.1586128>
- 773 Fernández R, Yamin L, Reyes JC, et al (2021) Mitigación del riesgo sísmico de la infraestructura
774 escolar. In: *Investigaciones en Gestión del Riesgo de Desastres para Colombia: Avances,*
775 *Perspectivas y Casos de Estudio*. Bogotá, pp 36–69
- 776 Fernández RI, Rincón R, Yamin LE (2019) Incertidumbre en el Beneficio Obtenido para Opciones
777 de Reforzamiento Sísmico. In: *IX Congreso Nacional de Ingeniería Sísmica*. Cali, Colombia
- 778 GEER (2017) Geotechnical Engineering Reconnaissance Of The 19 September 2017 Mw 7.1 Puebla-
779 Mexico City Earthquake Version 1.0. *Geotech Extrem Events Reconnaiss* GEER-055A:1–91.
780 <https://doi.org/10.18118/G6JD46>
- 781 GEER (2016) GEER-ATC earthquake reconnaissance April 16th 2016, Muisne, Ecuador. *Geotech*
782 *Extrem Events Reconnaiss Assoc Rep* GEER-049 604
- 783 Gehl P, Douglas J, Rossetto T, et al (2014) Investigating the Use of Record-to-Record Variability in
784 Static Capacity Approaches. *Proc 2nd Int Conf Vulnerability Risk Anal Manag ICVRAM 2014*
785 *6th Int Symp Uncertain Model Anal ISUMA 2014* 1675–1684.
786 <https://doi.org/10.1061/9780784413609.168>
- 787 Giordano N, De Luca F, Sextos A (2020) Out-of-plane closed-form solution for the seismic
788 assessment of unreinforced masonry schools in Nepal. *Eng Struct* 203:109548.
789 <https://doi.org/10.1016/j.engstruct.2019.109548>
- 790 Gogus A, Wallace JW (2015) Seismic Safety Evaluation of Reinforced Concrete Walls through
791 FEMA P695 Methodology. *J Struct Eng* 141:04015002. [https://doi.org/10.1061/\(asce\)st.1943-541x.0001221](https://doi.org/10.1061/(asce)st.1943-541x.0001221)

- 793 González C, Niño M, Jaimes MA (2020) Event-based assessment of seismic resilience in Mexican
794 school buildings. *Bull Earthq Eng* 18:6313–6336. <https://doi.org/10.1007/s10518-020-00938-5>
- 795 Gunasekera R, Ishizawa O, Aubrecht C, et al (2015) Developing an adaptive global exposure model
796 to support the generation of country disaster risk profiles. *Earth-Science Rev* 150:594–608.
797 <https://doi.org/10.1016/j.earscirev.2015.08.012>
- 798 Han S, Chopra AK (2006) Approximate incremental dynamic analysis using the modal pushover
799 analysis procedure. *Earthq Eng Struct Dyn* 1853–1873
- 800 Hosseinpour F, Abdelnaby AE (2017) Fragility curves for RC frames under multiple earthquakes.
801 *Soil Dyn Earthq Eng* 98:222–234. <https://doi.org/10.1016/j.soildyn.2017.04.013>
- 802 IADB (2014) Learning in Twenty-First Century Schools
- 803 Ibarra LF, Medina RA, Krawinkler H (2005) Hysteretic models that incorporate strength and stiffness
804 deterioration. *Earthq Eng Struct Dyn* 34:1489–1511. <https://doi.org/10.1002/eqe.495>
- 805 Kiureghian A Der, Ditlevsen O (2009) Aleatory or epistemic? Does it matter? *Struct Saf* 31:105–112.
806 <https://doi.org/10.1016/j.strusafe.2008.06.020>
- 807 Kreslin M, Fajfar P (2012) The extended N2 method considering higher mode effects in both plan
808 and elevation. *Bull Earthq Eng* 10:695–715. <https://doi.org/10.1007/s10518-011-9319-6>
- 809 Li Q, Ellingwood BR (2005) Structural response and damage assessment by enhanced uncoupled
810 modal response history analysis. *J Earthq Eng* 9:719–737
- 811 Magliulo G, Maddaloni G, Cosenza E (2012) Extension of N2 method to plan irregular buildings
812 considering accidental eccentricity. *Soil Dyn Earthq Eng* 43:69–84.
813 <https://doi.org/10.1016/j.soildyn.2012.07.032>
- 814 Mander JB, Priestley MJ., Park R (1988) Theoretical stress-strain model for confined concrete. *J*
815 *Struct Eng* 114:1804–1826
- 816 Masi A (2003) Seismic vulnerability assessment of gravity load designed R/C frames. *Bull Earthq*
817 *Eng* 1:371–395. <https://doi.org/10.1023/B:BEEE.0000021426.31223.60>
- 818 Michel C, Lestuzzi P, Lacave C (2014) Simplified non-linear seismic displacement demand
819 prediction for low period structures. *Bull Earthq Eng* 12:1563–1581.
820 <https://doi.org/10.1007/s10518-014-9585-1>
- 821 Miranda E (1999) Approximate seismic lateral deformation demands in multistory buildings. *J Struct*
822 *Eng* 125:417–425
- 823 Miranda E, Akkar SD (2006) Generalized Interstory Drift Spectrum. *J Struct Eng* 132:840–852.
824 [https://doi.org/10.1061/\(asce\)0733-9445\(2006\)132:6\(840\)](https://doi.org/10.1061/(asce)0733-9445(2006)132:6(840))
- 825 Mora MG, Valcárcel JA, Cardona OD, et al (2015) Prioritizing interventions to reduce seismic
826 vulnerability in school facilities in Colombia. *Earthq Spectra* 31:2535–2552.
827 <https://doi.org/10.1193/040412EQS151T>
- 828 Mwafy AM, Elnashai AS (2001) Static pushover versus dynamic collapse analysis of RC buildings.
829 *Eng Struct* 23:407–424. [https://doi.org/10.1016/S0141-0296\(00\)00068-7](https://doi.org/10.1016/S0141-0296(00)00068-7)
- 830 Nakashima M, Ogawa K, Inoue K (2002) Generic frame model for simulation of earthquake
831 responses of steel moment frames. *Earthq Eng Struct Dyn* 31:671–692.
832 <https://doi.org/10.1002/eqe.148>

- 833 Nassirpour A, Galasso C, D’Ayala D (2018) Increasing Seismic Resilience of Philippines’ School.
834 In: 16th European Conference on Earthquake Engineering. pp 1–12
- 835 PEER (2020a) Strong Ground Motion Databases. [https://peer.berkeley.edu/peer-strong-ground-](https://peer.berkeley.edu/peer-strong-ground-motion-databases)
836 [motion-databases](https://peer.berkeley.edu/peer-strong-ground-motion-databases)
- 837 PEER (2020b) OpenSees - The Open System for Earthquake Engineering Simulation
- 838 Porter KA, Beck JL, Shaikhutdinov R V. (2002) Sensitivity of building loss estimates to major
839 uncertain variables. *Earthq Spectra* 18:719–743. <https://doi.org/10.1193/1.1516201>
- 840 Prasad JSR, Singh Y, Kaynia AM, Lindholm C (2009) Socioeconomic clustering in seismic risk
841 assessment of urban housing stock. *Earthq Spectra* 25:619–641.
842 <https://doi.org/10.1193/1.3158547>
- 843 Qu Z, Gong T, Li Q, Wang T (2019) Evaluation of the fishbone model in simulating the seismic
844 response of multistory reinforced concrete moment-resisting frames. *Earthq Eng Eng Vib*
845 18:315–330. <https://doi.org/10.1007/s11803-019-0506-9>
- 846 Reyes JC, Chopra AK (2011) Evaluation of three-dimensional modal pushover analysis for
847 unsymmetric-plan buildings subjected to two components of ground motion. *Earthq Eng Struct*
848 *Dyn* 1475–1494
- 849 Rincon R, Yamin L, Becerra A (2017) Seismic Risk Assessment of Public Schools and Prioritization
850 Strategy for Risk Mitigation. *16th World:12*
- 851 Rossetto T, Gehl P, Minas S, et al (2014) Sensitivity Analysis of Different Capacity Spectrum
852 Approaches to Assumptions in the Modeling, Capacity and Demand Representations.
853 *Vulnerability, Uncertainty, Risk* 1665–1674. <https://doi.org/10.1061/9780784413609.167>
- 854 Ruggieri S, Perrone D, Leone M, et al (2020) A prioritization RVS methodology for the seismic risk
855 assessment of RC school buildings. *Int J Disaster Risk Reduct* 51:101807.
856 <https://doi.org/10.1016/j.ijdrr.2020.101807>
- 857 Samadian D, Ghafory-Ashtiany M, Naderpour H, Eghbali M (2019) Seismic resilience evaluation
858 based on vulnerability curves for existing and retrofitted typical RC school buildings. *Soil Dyn*
859 *Earthq Eng* 127:105844. <https://doi.org/10.1016/j.soildyn.2019.105844>
- 860 Silva V (2019) Uncertainty and correlation in seismic vulnerability functions of building classes.
861 *Earthq Spectra* 35:1515
- 862 Silva V, Akkar S, Baker J, et al (2018) Current challenges and Future Trends in Analytical Fragility
863 and Vulnerability Modelling. *Earthq Spectra* 173:669–680
- 864 The World Bank (2019) Global Library for School Infrastructure (GLOSI) - Global Program for Safer
865 Schools. <https://gps.worldbank.org/en/GLOSI>. Accessed 10 Oct 2021
- 866 The World Bank (2018) Información Técnica para el Plan de Mitigación del Riesgo Sísmico de las
867 Edificaciones Escolares en El Salvador
- 868 The World Bank (2020) Evaluación del riesgo por sismo y viento huracanado y planes de reducción
869 del riesgo para la infraestructura educativa pública de República Dominicana
- 870 UNDRR (2017) Comprehensive School Safety, A global framework in support of The Global
871 Alliance for Disaster Risk Reduction and Resilience in the Education Sector and The Worldwide
872 Initiative for Safe Schools. Geneva, Switzerland

- 873 UNESCO (2019) Guidelines for Assessing Learning Facilities in the Context of Disaster Risk
874 Reduction and Climate Change Adaptation. Volume 1 - Introduction to learning facilities
875 assessment and to the VISUS methodology. Paris, France
- 876 United Nations (2015) Sustainable Development Goals. <https://sustainabledevelopment.un.org>
- 877 Vamvatsikos D, Cornell CA (2002) Incremental dynamic analysis. 514:491–514.
878 <https://doi.org/10.1002/eqe.141>
- 879 Vatteri AP, D’Ayala D (2021) Classification and seismic fragility assessment of confined masonry
880 school buildings. Bull Earthq Eng 19:2213–2263. <https://doi.org/10.1007/s10518-021-01061-9>
- 881 Wald DJ, Allen TI (2007) Topographic slope as a proxy for seismic site conditions and amplification.
882 Bull Seismol Soc Am 97:1379–1395. <https://doi.org/10.1785/0120060267>
- 883 Wen YK, Ellingwood BR, Veneziano D, Bracci J (2003) Uncertainty modeling in earthquake
884 engineering. MAE Cent Proj 1–113
- 885 Yamin LE, Hurtado A, Rincon R, et al (2017) Probabilistic seismic vulnerability assessment of
886 buildings in terms of economic losses. Eng Struct 138:308–323.
887 <https://doi.org/10.1016/j.engstruct.2017.02.013>
- 888 Yamin LE, Hurtado AI, Barbat AH, Cardona OD (2014) Seismic and wind vulnerability assessment
889 for the GAR-13 global risk assessment. Int J Disaster Risk Reduct 10:452–460.
890 <https://doi.org/10.1016/j.ijdr.2014.05.007>

891

892 **Declarations**

893 This study was developed under the Global Program for Safer Schools (GPSS), funded by the Global
894 Facility for Disaster Reduction and Recovery (GFDRR) of The World Bank.